water

MDPI

*Article*

# Interactions Evaluation between the Jouamaa Hakama Groundwater and Ouljat Echatt River in the North of Morocco, Using Hydrochemical Modeling, Multivariate Statistics and GIS

**El Mustapha Azzirgue [1], El Khalil Cherif [2,3,4,*], Hamza El Azhari [1], Houria Dakak [5], Hasna Yachou [5], Ahmed Ghanimi [6], Nordine Nouayti [7], Joaquim Esteves da Silva [8,*] and Farida Salmoun [1]**

[1] Laboratory of Physical Chemistry of Materials, Natural Substances and Environment, Chemistry Department, Sciences and Technology Faculty, Abdelmalek Essaâdi University, Tangier 90090, Morocco
[2] Institute for Systems and Robotics, Instituto Superior Técnico, University of Lisbon, 1649-004 Lisbon, Portugal
[3] National Institute of Oceanography and Applied Geophysics (OGS), Centre for Management of Maritime Infrastructure (CGN), Borgo Grotta Gigante 42/C, Sgonico, 34010 Trieste, Italy
[4] MARETEC—Marine, Environment and Technology Center, Instituto Superior Tecnico, Universidade de Lisboa, Av. Rovisco Pais 1, 1049-001 Lisboa, Portugal
[5] Research Unit on Environment and Conservation of Natural Resources, Regional Center of Rabat, National Institute of Agronomic Research (INRA), Av. Ennasr, Rabat 10100, Morocco
[6] Laboratory of Materials, Nanotechnology and Environment, Faculty of Sciences Rabat, Mohammed V University in Rabat, Rabat 10101, Morocco
[7] Environmental Management and Civil Engineering Team, Laboratory of Applied Sciences, National School of Applied Sciences, Abdelmalek Essaadi University, Al Hoceima 32002, Morocco
[8] Centro de Investigação em Química (CIQUP), Instituto de Ciências Moleculares (IMS), Departamento de Geociências, Ambiente e Ordenamento do Território, Faculdade de Ciências, Universidade do Porto, Rua do Campo Alegre s/n, 4169-007 Porto, Portugal
* Correspondence: c.elkhalil@uae.ac.ma (E.K.C.); jcsilva@fc.up.pt (J.E.d.S.)

**Abstract:** The processed discharges from Tangier Automotive City's (TAC) Chrafate Wastewater Treatment Plant (WWTP) contaminate the Jouamaa Hakama groundwater and the Ouljat Echatt river. We aimed to study the unknown interactions between surface water (SW) and groundwater (GW). A total of nine Jouamaa Hakama GW samples and eleven Ouljat Echatt SW samples were taken and analyzed in 2021 and 2022 to determine 16 physical and chemical parameters (pH, temperature (T), electrical conductivity (EC), dissolved oxygen (DO), total hardness (TH), turbidity (TURB), and total dissolved solids (TDS), cations: $Na^+$, $K^+$, $Mg^{2+}$ and $Ca^{2+}$, anions: $Cl^-$, $CO_3{}^{2-}$, $HCO_3{}^-$, $NO_3{}^-$, and $SO_4{}^{2-}$). For exploitation of the data, we used a methodology based on hydrochemical modeling (HM), principal component analysis (PCA), Water Quality Index (WQI), Irrigation Water Quality Index (IWQI), inverse distance weighted interpolation (IDW) using Geographic Information Systems (GIS), and regression analysis (RA). We studied the interaction of the surface water of the river (contaminated by discharges from the WWTP) with the shallow groundwater on a strip of 100 m on either side of the river to understand the transverse and longitudinal dispersion of this pollution The investigations indicated that the major ions found in GW and SW were characterized in a different order in the anion list order $Cl^- > CO_3{}^{2-} > NO_3{}^- > HCO_3{}^- > SO_4{}^{2-}$ and $Cl^- > SO_4{}^{2-} > CO_3{}^{2-} > NO_3{}^- > HCO_3{}^-$, respectively, while the concentrations of cations showed the same order for both: $Na^+ > Ca^{2+} > Mg^{2+} > K^+$. As a result, GW showed in the Piper diagram the type of sodium chloride to magnesium carbonate, while SW belongs to the sodium chloride to magnesium sulfate type. The WQI showed that the river waters are all unsuitable for use (WQI > 100), while the GW is of poor quality (WQI > 76). Moreover, the results of the GW–SW interaction along the river revealed a significant relationship ($R^2$ = 0.85), which means that strong circulation and the infiltration of contaminated SW into shallow GW occur in this area. The approaches followed have been proven effective in evaluating water quality for human and animal uses. These results can help decision-makers in the region take suitable management measures to mitigate this environmental problem.



**Citation:** Azzirgue, E.M.; Cherif, E.K.; El Azhari, H.; Dakak, H.; Yachou, H.; Ghanimi, A.; Nouayti, N.; Esteves da Silva, J.; Salmoun, F. Interactions Evaluation between the Jouamaa Hakama Groundwater and Ouljat Echatt River in the North of Morocco, Using Hydrochemical Modeling, Multivariate Statistics and GIS. *Water* **2023**, *15*, 1752. https://doi.org/10.3390/w15091752

Academic Editor: Paolo Fabbri

Received: 16 March 2023
Revised: 22 April 2023
Accepted: 24 April 2023
Published: 2 May 2023

**Keywords:** North of Morocco; GW–SW interaction; hydro-geochemistry quality; PCA; GIS; IDW

## 1. Introduction

The irrational use of freshwater and water stress caused by climate changes have added to pollution of water by various anthropogenic activities, leading to the degradation of ecosystems and biodiversity essential for human needs [1–3]. Freshwater is a limited and fragile asset, threatened by growing consumption and multiple forms of pollution. It is also an essential non-renewable natural resource that must be preserved [3]. Most surface water (SW), such as rivers, are connected to groundwater (GW) [4,5]. Indeed, the dynamics of exchanges and river–aquifer interactions include the infiltration of solutes from river waters which leads to the reconstitution and recharge of GW through these SW masses, thus producing variations in the quality of GW [6].

Additionally, urban growth leads to large municipal landfills and wastewater contamination of nearby waterways, especially GW and SW. This leads to questions about the nature of these water resources, as GW contamination persists for a long time due to the slow movement of water [7]. This is why it is important to ensure that the quality of freshwater is secure for use by humans [8]. Morocco, like all the other countries in the world, is affected by climate change and freshwater pollution. Thus, ongoing management is required to safeguard water resources. It is critical to conduct quality monitoring of GW and SW used for consumption in order to safeguard their quality [9]. Therefore, physico-chemical [10,11], hydrochemical [12], and bacteriological [13] factors can be used to evaluate the freshwater quality. However, analysis of GW and SW quality parameters are costly and time-consuming. To improve freshwater quality, it is very important to interpret different variations in freshwater quality [14] and to locate hidden sources of contamination [15–17]. For that purpose, to characterize the quality of SW, several researchers have used pertinent methods and techniques, such as WQI, which is regarded as one of the most efficient techniques for assessing water quality [18–20]. Moreover, fuzzy logic [21,22], machine learning [23,24], and the projection pursuit approach [11,25,26] have been used to forecast dam water quality [23], river water quality, and GW quality [11,25,26], and neural networks have been utilized to analyze water quality [27,28]. Multivariate statistical approaches can be used to assess large freshwater quality datasets with a minimum loss of information [29,30], which is valuable for quickly characterization of the contamination [31,32]. Some researchers [33–36] have combined GIS techniques with multivariate statistical approaches to define freshwater quality; others have combined statistical techniques, GIS, and WQI. Many scientists have investigated the properties of water hydrochemistry and the main mechanisms of regulation of freshwater hydrochemistry [37–40]. The use of the Piper diagram helps to determine the chemical parameters of GW [41] and SW [12]. Some researchers used PCA to complement diagrams such as Wilcox, Riverside, Stiff, Schöeller Berkaloff, Piper, and Durov plots [42–45]. Therefore, the integration of hydrochemical, PCA, and GIS techniques [46] or the integration of hydrochemical, WQI, and PCA techniques could help to study the origin, evolution, and interaction processes [47–49].

GW and SW are interconnected in a river basin [5], where they mix with longitudinal and transverse flows [50]. These GW–SW interactions result in high biogeochemical activity, chemical transformations, and GW contamination if the SW is polluted [51–53]. Understanding the interactions between SW and GW is of paramount importance for the monitoring and control of water resources and the protection of ecosystems [54]. For that, several methods were developed to study GW–SW interaction patterns [55–57]. As a result, the combination of different approaches is recommended and highlighted in recent studies [58,59], with the aim to protect water resources and understand the parameters and processes influencing the GW–SW interaction [60,61].

In Morocco, several studies have been carried out on seawater intrusion in GW [62–66], while other studies have been carried out on assessment of GW quality and recharge mechanisms [67], and prediction of the WQI for the GW with multi-layer perceptron approaches [68]. However, few studies have been carried out on GW–SW interaction models [69]. As a result, the goals of this work were to combine hydrochemical, WQI, IWQI, PCA, and GIS-based (IDW) interpolation to describe the geographical interaction of SW and GW hydrochemistry and to uncover spatial patterns. In our work, the GW and SW quality was assessed on water samples from wells and rivers in the study area and on 16 parameters from 20 sampling sites in order to evaluate spatial variations in GW and SW. This study seeks to assist water authorities and managers in establishing priorities, making informed decisions to improve the quality of GW and SW.

This research is an exploratory study, the first in the area, in which we have tried to investigate the interaction of the surface water of the river contaminated by discharges from the wastewater treatment plants (WWTP) with the shallow groundwater on a strip of 100 m on either side of the river to understand the transverse and longitudinal dispersion of this pollution. The Ouljat Echatt river is a concern for decision-makers, and implementing this study is considered an innovation for the management of water quality in the region. We can also apply it to other regions with similar conditions for maintaining the principles of sustainable development.

## 2. Materials and Methods

### *2.1. Study Area*

Tangier-Tetouan-Al Hoceima is in northwest of Morocco. It is one of the twelve regions of the Kingdom of Morocco. Its capital is Tangier-Assilah. The region covers an area of 17,262 km$^2$, representing 2.43% of the national territory. The Tangier-Tetouan-Al Hoceima region retains its place among the leading growth regions, marking a growth rate higher than the national average [70]. Far from the city of Tangier, about 17 km on the national road number 2, is the study site. It includes the Ouljat Echatt river which passes next to the municipality of Hakama, as well as GW on either side of the river downhill of the WWTP discharges [10,11,22]. This WWTP treats effluents rejected by the industrial zone of Tangier Automotive City (Figures 1 and 2).

### *2.2. Climate*

The climate in the north of Morocco is of subhumid Mediterranean type; the winter is humid and mild, and the summer is dry and hot [11]. Average rainfall in the Tangier-Tetouan-Al Hoceima region is around 700 mm; the wettest year was 1963 with a height of 1248 mm, while the driest year was 1973 with only 412 mm. Moreover, the importance of occult precipitation, such as fog, mist, dew which softens the climate outside the wet season, should be noted.

### *2.3. Geology and Hydrogeology*

The research region belongs to the geological section of the Rif domain, with flysch nappes in the exterior Rif, which is depicted in this region by the Tangier unit. This is the flysch nappe substratum. The research area comprises flysch outcrops, extensive outcrops of the predominantly clayey Tangier unit, which is part of the external Rif, and some mainly alluvial quaternary formation strategies to alleviate this environmental issue [71].

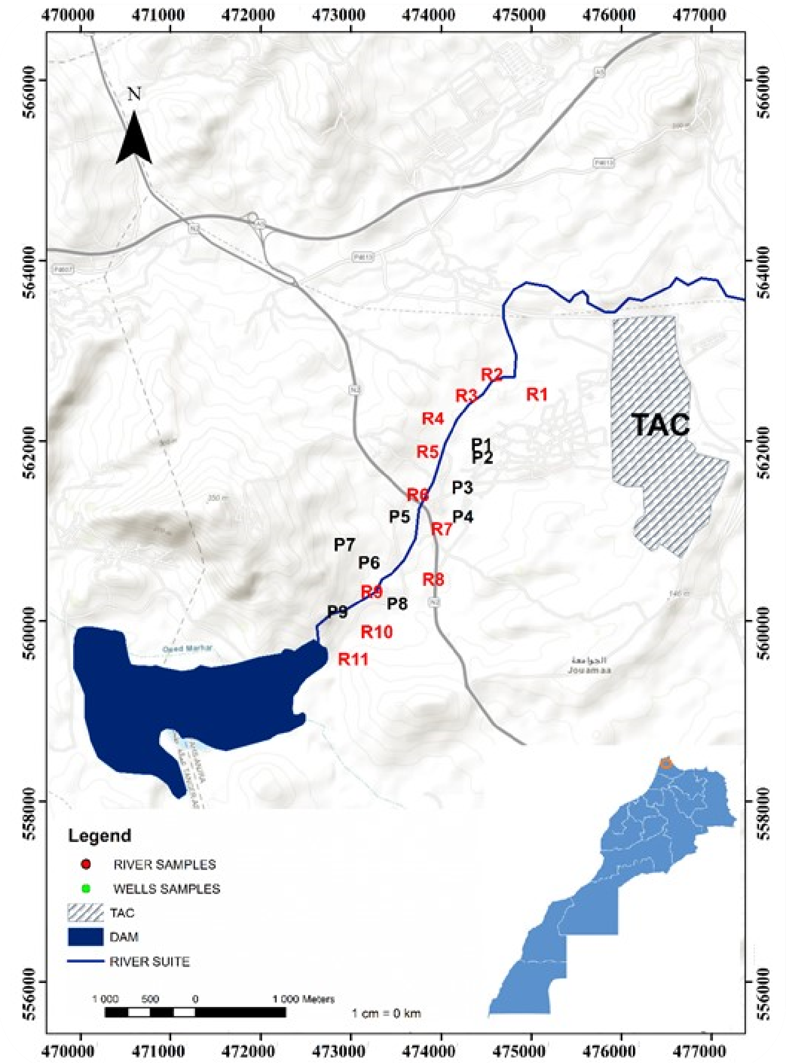


**Figure 1.** The situation of the study zone and the surveyed station.

**Figure 2.** *Cont.*

**Figure 2.** Sampling sites of water points in the watershed.

*2.4. Sampling, Laboratory Analysis and Analytical Method*

During the years 2021 and 2022, sampling was carried out in the research region (Figures 1 and 2). There were nine GW samples and eleven SW samples collected, as well as 16 physical and chemical parameters assessed. The samples were identified using technical sampling sheets (date, time of sampling, number, and Lambert coordinates). Table 1 presents the geographic coordinates of the sampling sites.

**Table 1.** Geographic coordinates of river and wells samples.

| Points | Long | Lat |
|---|---|---|
| R1 | −5.67463746° | 35.66688479° |
| R2 | −5.67766835° | 35.66541206° |
| R3 | −5.68093907° | 35.66351440° |
| R4 | −5.68364274° | 35.66088328° |
| R5 | −5.68626245° | 35.65523154° |
| R6 | −5.68576545° | 35.65334556° |
| R7 | −5.68819553° | 35.65227545° |
| R8 | −5.68982623° | 35.64715242° |
| R9 | −5.69294471° | 35.64394728° |
| R10 | −5.69726585° | 35.64224707° |
| R11 | −5.70137617° | 35.63777176° |
| P1 | −5.68275827° | 35.66043753° |
| P2 | −5.68265338° | 35.66000167° |
| P3 | −5.68549656° | 35.65540978° |
| P4 | −5.68530379° | 35.65319523 ° |
| P5 | −5.68832221° | 35.65258791° |
| P6 | −5.68988600° | 35.64719612° |
| P7 | −5.69093475° | 35.64789468° |
| P8 | −5.69290863° | 35.64402414° |
| P9 | −5.69721983° | 35.64247992° |

The stations for sampling were chosen with little variation. While the sample was collected in temperatures ranging from 0 to 4 degrees Celsius were used for transportation and storage [72]. Temperature, pH, DO, Turb, and EC analysis were measured in situ to prevent any modification of the sample parameters. Table 2 presents parameters measured for each sample and the used analytical methods [73].

**Table 2.** List of the in situ and laboratory analysis.

| Parameters | Analytical Method | Unit | Maximum Allowable Values WHO | Moroccan Standard [74,75] |
|---|---|---|---|---|
| pH | pH meter | — | 6.5 < pH < 8.5 | 6.5 < pH < 9 |
| T | Thermometer | °C | T° < 25 | T° < 30 |
| EC | Conductimeter | µS/cm | 2700 | 2700 |
| DO | Oximeter | mg/L | $5 < O_2 < 8$ | $5 < O_2 < 8$ |
| TURB | Turbidimetry | NFU | 5 | 5 |
| $Ca^{2+}$ | Titrimetric technique | mg/L | 75 | 75 |
| $Mg^{2+}$ | Complexometry with E.D.T.A. (0.02 N) | mg/L | 50 | 50 |
| $Na^+$ | Flame photometer | mg/L | 200 | 200 |
| $K^+$ | photometer | mg/L | 50 | 50 |
| $Cl^-$ | Mohr's method | mg/L | 250 | 300 |
| $HCO_3{}^-$ | Acido-basic titration (HCl 0.05 N) | mg/L | 120 | 120 |
| $CO_3{}^{2-}$ | | mg/L | 100 | 100 |
| $NO_3{}^{2-}$ | Steam distillation | mg/L | 50 | 50 |
| $SO_4{}^{2-}$ | Nephelometric method | mg/L | 250 | 200 |
| TDS | | mg/L | 500 | 500 |
| TH | | mg/L | 400 | 400 |

For the study of the GW–SW interaction, we exploited the data and adopted a methodology based on hydrochemical modeling, PCA, WQI, irrigation indices, GIS-based Inverse Distance Weighted Interpolation, and regression analysis. Figure 3 shows the distances between the wells and the river boundary.

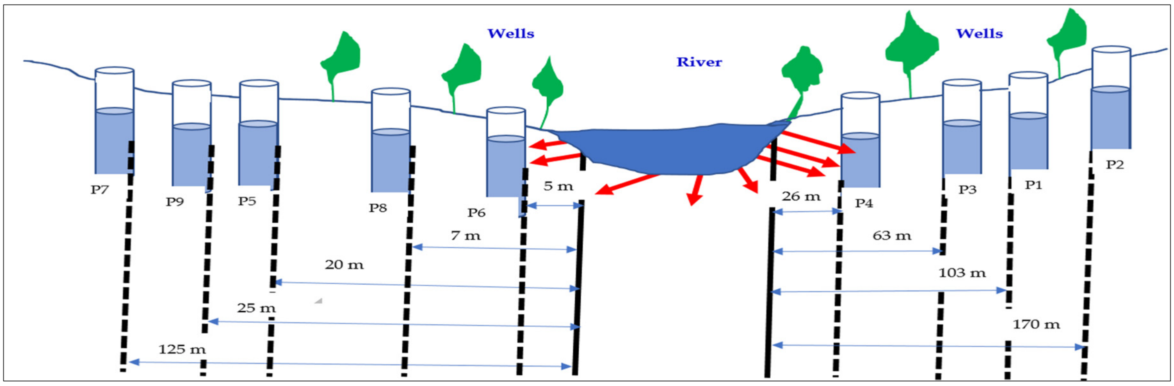


**Figure 3.** Schematic section showing the distances between the wells and the river boundary.

## 2.5. Water Quality Index (WQI)

Studies have used freshwater quality evaluation techniques [19,76], and the WQI is a simple and efficient method [12,17,22,77–79]. The WQI explains water quality using a number of indices that reflect water quality for users and consumers [80]. The WQI can be used for GW (GWQI) [22] or for SW (SWQI) [12]. When developing a WQI, the importance of different parameters affecting water quality depends on the intended water use [81].

The WQI has the advantage of minimizing the number of water parameters used in an assessment and providing a single value. This value is a simplified and logical expression that expresses the average quality of water at a specific time based on the analytical values of physico-chemical parameters.

In this study, the estimates of the GWQI and SWQI were based on the suitability of the samples for consumption and other household uses.

The WQI calculations involved the following steps. First, the sixteen analyzed parameters were weighted (wi) according to their importance in drinking water quality assessments. The parameters were weighted between 1 and 4 according to their importance in drinking water assessments, such as knowledge of the hydrological framework of the study area, while taking into account macronutrients [82].

The arithmetic weighted index (WQI) was used to calculate the results in this paper. This approach assigns weight to chemical characteristics based on subjective criteria [83]. The WQI was calculated in five phases, as stated below [84]:

The relative weights (Wi) for each of the parameters were estimated (Equation (1)).

$$\mathrm{Wi} = \frac{\mathrm{wi}}{\sum_{k=0}^{n} \mathrm{wi}} \quad (1)$$

The quality score was determined (Equation (2)):

$$\mathrm{Qi} = \frac{\mathrm{Ci}}{\mathrm{Si}} \times 100 \quad (2)$$

The Qi was calculated according to Equation (3):

$$\mathrm{Qi} = \frac{(\mathrm{CpH} - 8.5)}{(6.5 - 8.5)} \quad (3)$$

"SI" was calculated following Equation (4).

$$\mathrm{SI} = \mathrm{Wi} \times \mathrm{Qi} \quad (4)$$

The WQI was calculated with Equation (5):

$$\mathrm{WQI} = \sum_{k=1}^{n} \mathrm{Wi} \times \mathrm{Qi} = \sum_{1}^{n} \mathrm{SI} \quad (5)$$

According to the calculated GWQI and SWQI value [85], the GW and SW quality is shown in Table 3.

**Table 3.** The WQI categories [86].

| Classes | Classification |
|---|---|
| 0 to 25 | Excellent |
| 26 to 50 | Good |
| 51 to 75 | Poor |
| 76 to 100 | Very poor |
| >100 | Unsuitable for drinking |

### *2.6. Water for Irrigation Use (IWQI)*

Water quality is thus an important element in the sustainable use of water for irrigation, particularly in cases where salinity development is expected to be a problem in an irrigated agricultural area. The hydrochemical characteristics of the main GW and SW variables are used in this evaluation to determine the suitability for irrigation [87]. The next paragraph provides a number of calculations that may assist in establishing the suitability of irrigation water.

Equation (6) was used to calculate the sodium adsorption rate SAR [87], which is defined as the salt risk associated with calcium and magnesium concentrations [88].

$$\mathrm{SAR} = \frac{\mathrm{Na}^{+}}{\sqrt{\frac{\mathrm{Ca}^{2+} + \mathrm{Mg}^{2+}}{2}}} \quad (6)$$

$$\mathrm{RSC} = \left[\left(\mathrm{HCO_3}^{-} + \mathrm{CO_3}^{-}\right) - \left(\mathrm{Ca}^{2+} + \mathrm{Mg}^{2+}\right)\right] \quad (7)$$

$$Na\% = \frac{(Na^{+} + K^{+}) * 100}{\left(Ca^{2+} + Mg^{2+} + Na^{+} + K^{+}\right)} \tag{8}$$

$$MH = \frac{\left(Mg^{2+} * 100\right)}{\left(Ca^{2+} + Mg^{2+}\right)} \tag{9}$$

$$PI = \frac{\left(Na^{+} + \sqrt{HCO_3{}^{-}}\right) * 100}{\left(Ca^{2+} + Mg^{2+} + Na^{+}\right)} \tag{10}$$

$$KI = \frac{Na^{+}}{Ca^{2+} + Mg^{2+}} \tag{11}$$

$$PS = Cl^{-} + \frac{1}{2} SO_4{}^{2-} \tag{12}$$

$$RSBC = HCO_3{}^{-} - Ca^{2+} \tag{13}$$

Equation (7) was used to calculate the RSC, which plays an important part of irrigation water. In addition, there is another approach, which is widely used to understand the effects of excess calcium and magnesium on soil [89]. The risk of magnesium (MH) (Equation (9)), and the percentage of sodium (%Na) (Equation (8)), are important parameters that can be used to evaluate the quality of GW and its appropriateness for irrigation purposes. A well-known classification was developed by Wilcox [90], which has been documented and used in the literature for a long time. The GW and SW were classified into five classes of Equations (8) and (9) [91]. PI is an index for the permeability of water in soil (Equation (10)) [92].

Sodium, when compared to $Ca^{2+}$ and $Mg^{2+}$, KI > 1 indicates an excess of salt, whereas a KI < 2 indicates a shortfall in water (Equation (11)) [88]. Salinity potential (PS) (Equation (12)) refers to the quantity of salt that builds up in the soil, which is constantly dissolved in irrigation water, increasing salinity as determined by the formula below [88]. Since most natural waters do not have substantial levels of carbonate ions and bicarbonate ions do not precipitate magnesium ions, the alkalinity hazard was measured by an indicator known as residual sodium bicarbonate (RSBC) and calculated using (Equation (13), Table 4) [89].

**Table 4.** Calculating irrigation quality parameters and classification of water.

| Parameters | Classification | References |
|---|---|---|
| SAR | Excellent, Good, Permissible, Doubtful | [93] |
| RSC | Good, Medium, Bad | [94] |
| Na% | Excellent, Good, Permissible, Doubtful, Unsuitable | [90] |
| PI | Excellent, Good, Unsuitable | [95] |
| KI | Permissible, Non- Permissible | [96] |
| PS | Excellent, Good, | [95] |
| RSBC | Excellent, Good, | [97] |
| MH | Suitable, Unsuitable, | [98] |

### *2.7. Multivariate Statistical Analysis (MSA) and the Geological Information System (GIS)*

Our work examined 16 physical-chemical parameters from 9 wells and 11 source sites from the Ouljat Echatt river, including: pH, T, EC, DO, TH, TURB, TDS, cations: $K^{+}$, $Na^{+}$, $Ca^{2+}$, $Mg^{2+}$, and anions: $Cl^{-}$, $HCO_3{}^{-}$, $CO_3{}^{2-}$, $NO_3{}^{-}$, $SO_4{}^{2-}$, which are used for PCA [99].

We used the program Arc GIS 10.6.1 for data input, analysis, and mapping. This method originated in mining and geological engineering based on locations weighted only by distance [100,101]. The value obtained from the known location was used to estimate the value of a variable at some new locations.

The IDW approach was implemented using ArcGIS 10.6's Spatial Analyst Extension. The experimental results from the laboratory study of water samples collected from well sites and along the river were combined into an Excel file, which was then translated into a shapefile. The overage of the data found from the measured sites for each parameter was applied in the numerical calculation of each interpolated cell, and the river network was used for the mask. On the output raster, the cells corresponding to the Ouljat Echatt watershed region became the values of the first input raster. Water quality classifications were based on the geographic distribution of pollutants, with a map legend based on each parameter's data range. IDW interpolation is a technique that is largely used in the mapping of variables. It is an exact and convex interpolation method that fits only the continuous model of spatial variation. This method is based on locations weighted only by distance. The value obtained from the known location was used to estimate the value of a variable at some new locations.

## 3. Results and Discussion

### 3.1. Hydrochemical Data Correlation

Understanding freshwater hydrochemical characteristics is crucial for the preservation of the water resources in this work, and the chemical elements of freshwaters are considered valuable information on the suitability of various uses. We sought to assess the quality of GW–SW based on the distribution of cations and anions in GW–SW downstream of treated wastewater discharges from the TAC industrial zone. The hydrochemical characteristics of the GW of the Jouamaa Hakama site and Ouljat Echatt River water showed variable hydrochemical characteristics.

The pH of GW values was between 7.79 and 6.91, while the waters of the Ouljat Echatt River had a pH between 7.31 and 6.9. The average pH of GW was 7.38, which is higher than that of SW (pH = 7.10). The EC values of the GW were between 806 μS/cm and 1337 μS/cm, with a mean value of 1768 μS/cm, while SW values were between 878 μS/cm and 1205 μS/cm with an average of 1089.36 μS/cm. EC values of surface and groundwater were higher than the WHO limit of 1000 μS/cm in some samples.

The TSD values of GW were between 515.84 mg/L and 1131.52 mg/L with an average of 855.68 mg/L, while SW values were between 561.92 mg/L and 771.2 mg/L with an average of 697.19 mg/L (Table 4). The $Cl^-$ values of GW and river water averaged around 205.1 and 153.5 mg/L, respectively. GW and river water $NO_3^-$ values averaged around 26 and 28.9 mg/L, respectively. GW and river water $SO_4^{2-}$ values averaged around 82.3 and 71.8 mg/L, respectively (Table 5).

GW $HCO_3^-$ concentration values were between 7.6 and 30.5 mg/L with an average of 13.6, while the concentration at SW were between 7.6 and 15.3 with an average of 8.3. GW $CO_3^{2-}$ values were between 26.3 and 93.8 with an average of 62.1 while SW values were between 37.5 and 78.8 with an average of 64.1 (Tables 5 and 6). GW $Ca^{2+}$ values were between 16 and 80 with an average of 50.2 mg/L while SW values were between 32 and 52 with an average of 41.8 mg/L. GW $Mg^{2+}$ values were between 24 and 50.4 with an average of 36.3 mg/L while SW values were between 10.8 and 21.6 with an average of 16.3 mg/L. The GW $Na^+$ values were between 55.5 and 135.5 with the average of 100.2 mg/L while the SW values were between 71.2 and 135.5 and the average was 112.4 mg/L. GW $K^+$ values were between 0.4 and 5.1 and with a mean of 2.3 mg/L while SW values were between 7.5 and 12.5 and with a mean of 10.1 mg/L (Tables 5 and 6). The orders of major cations and anions in GW were $Cl^- > CO_3^{2-} > NO_3^- > HCO_3^- > SO_4^{2-}$ for anions and $Na^+ > Mg^{2+} > Ca^{2+} > K^+$ for cations. At the same time, the orders in the water of the Ouljat Echatt River were $Cl^- > SO_4^{2-} > CO_3^{2-} > NO_3^- > HCO_3^-$ for anions and $Na^+ > Ca^{2+} > Mg^{2+} > K^+$ for cations.

**Table 5.** The physicochemical measurement results of 20 sampling river.

| Sampling | T | EC | TDS | pH | DO (mg/L) | $Ca^{2+}$ (mg/L) | $Mg^{2+}$ (mg/L) | $Na^{+}$ (mg/L) | $K^{+}$ (mg/L) | $Cl^{-}$ (mg/L) | $HCO_3^{-}$ (mg/L) | $CO_3^{2-}$ (mg/L) | $NO_3^{-}$ (mg/L) | $SO_4^{2-}$ (mg/L) | TURB | TH |
|---|---|---|---|---|---|---|---|---|---|---|---|---|---|---|---|---|
| R1 | 17.00 | 1157.0 | 740.5 | 7.08 | 8.30 | 36.0 | 16.8 | 135.5 | 12.48 | 153.3 | 7.63 | 67.50 | 18.00 | 113.09 | 30.50 | 159.07 |
| R2 | 17.40 | 1205.0 | 771.2 | 7.17 | 6.82 | 44.0 | 16.8 | 126.6 | 11.80 | 152.3 | 7.63 | 78.75 | 18.00 | 96.31 | 45.20 | 179.05 |
| R3 | 20.10 | 1142.0 | 730.9 | 7.31 | 7.01 | 44.0 | 19.2 | 119.7 | 10.73 | 149.1 | 7.63 | 71.25 | 24.00 | 101.66 | 30.20 | 188.93 |
| R4 | 19.00 | 1072.0 | 686.1 | 6.91 | 7.00 | 44.0 | 16.8 | 114.7 | 9.75 | 148.1 | 7.63 | 56.25 | 36.00 | 96.38 | 21.50 | 179.05 |
| R5 | 18.60 | 1161.0 | 743.0 | 7.04 | 6.76 | 44.0 | 18.0 | 71.2 | 9.46 | 149.5 | 7.63 | 67.50 | 36.00 | 0.00 | 22.40 | 183.99 |
| R6 | 19.10 | 1188.0 | 760.3 | 7.09 | 6.11 | 52.0 | 15.6 | 128.6 | 10.34 | 151.2 | 7.63 | 56.25 | 30.00 | 140.88 | 19.00 | 194.08 |
| R7 | 20.30 | 1182.0 | 756.5 | 6.97 | 6.5 | 48.0 | 21.6 | 129.6 | 10.24 | 163.8 | 7.63 | 63.75 | 30.00 | 127.94 | 19.20 | 208.80 |
| R8 | 19.80 | 1061.0 | 679.0 | 7.08 | 6.4 | 40.0 | 10.8 | 117.7 | 10.73 | 160.0 | 7.63 | 71.25 | 30.00 | 34.66 | 20.10 | 144.35 |
| R9 | 20.10 | 1053.0 | 673.9 | 7.12 | 6.7 | 40.0 | 12.0 | 123.6 | 10.92 | 144.6 | 7.63 | 67.50 | 30.00 | 79.20 | 17.60 | 149.30 |
| R10 | 20.50 | 884.0 | 565.8 | 7.09 | 6.2 | 32.0 | 18.0 | 87.0 | 7.70 | 152.6 | 7.63 | 67.50 | 30.00 | 0.00 | 17.80 | 154.03 |
| R11 | 20.70 | 878.0 | 561.9 | 7.20 | 7.4 | 36.0 | 13.2 | 82.1 | 7.51 | 164.5 | 15.25 | 37.50 | 36.00 | 0.00 | 16.90 | 144.25 |
| Average | 19.33 | 1089.36 | 697.19 | 7.10 | 6.8 | 41.8 | 16.3 | 112.4 | 10.1 | 153.5 | 8.3 | 64.1 | 28.9 | 71.8 | 23.67 | 171.4 |
| Max | 20.70 | 1205.0 | 771.2 | 7.31 | 8.3 | 52.0 | 21.6 | 135.5 | 12.5 | 164.5 | 15.3 | 78.8 | 36.0 | 140.9 | 45.20 | 208.8 |
| Min | 17.00 | 878.0 | 561.9 | 6.91 | 6.1 | 32.0 | 10.8 | 71.2 | 7.5 | 144.6 | 7.6 | 37.5 | 18.0 | 0.0 | 16.90 | 144.2 |

**Table 6.** The physicochemical measurement results of 20 sampling wells.

| Sampling | T | EC | TDS | pH | DO (mg/L) | $Ca^{2+}$ (mg/L) | $Mg^{2+}$ (mg/L) | $Na^{+}$ (mg/L) | $K^{+}$ (mg/L) | $Cl^{-}$ (mg/L) | $HCO_3^{-}$ (mg/L) | $CO_3^{2-}$ (mg/L) | $NO_3^{-}$ (mg/L) | $SO_4^{2-}$ (mg/L) | TURB | TH |
|---|---|---|---|---|---|---|---|---|---|---|---|---|---|---|---|---|
| P1 | 16.20 | 806.0 | 515.8 | 7.39 | 7.6 | 32.0 | 24.0 | 55.5 | 0.68 | 152.3 | 7.63 | 48.75 | 24.00 | 0.00 | 4.30 | 178.736 |
| P2 | 16.80 | 1262.0 | 807.7 | 6.91 | 6.3 | 32.0 | 36.0 | 98.9 | 0.39 | 231.0 | 7.63 | 37.50 | 36.00 | 16.08 | 4.10 | 228.152 |
| P3 | 17.30 | 824.0 | 527.4 | 6.92 | 6.5 | 16.0 | 24.0 | 72.2 | 2.15 | 189.4 | 7.63 | 26.25 | 24.00 | 0.00 | 3.40 | 138.784 |
| P4 | 16.90 | 1509.0 | 965.8 | 7.70 | 7.5 | 44.0 | 28.8 | 146.4 | 2.24 | 389.2 | 7.63 | 33.75 | 30.00 | 0.00 | 2.90 | 228.4664 |
| P5 | 17.20 | 1198.0 | 766.7 | 7.29 | 7.0 | 60.0 | 31.2 | 65.3 | 1.66 | 174.7 | 15.25 | 78.75 | 30.00 | 5.54 | 3.10 | 278.3016 |
| P6 | 18.50 | 1768.0 | 1131.5 | 7.39 | 6.8 | 80.0 | 44.4 | 191.9 | 4.49 | 171.9 | 22.88 | 78.75 | 36.00 | 367.06 | 3.30 | 382.5992 |
| P7 | 17.10 | 1355.0 | 867.2 | 7.79 | 6.3 | 56.0 | 50.4 | 117.7 | 2.24 | 197.1 | 15.25 | 75.00 | 18.00 | 167.74 | 5.40 | 347.3792 |
| P8 | 18.20 | 1688.0 | 1080.3 | 7.57 | 6.7 | 60.0 | 50.4 | 64.3 | 5.07 | 169.4 | 30.50 | 93.75 | 12.00 | 70.08 | 5.80 | 357.3672 |
| P9 | 18.10 | 1623.0 | 1038.7 | 7.44 | 7.6 | 72.0 | 37.2 | 90.0 | 1.56 | 170.8 | 7.63 | 86.25 | 24.00 | 113.90 | 5.90 | 332.9736 |
| Average | 17.37 | 1337.0 | 855.7 | 7.38 | 6.9 | 50.2 | 36.3 | 100.2 | 2.3 | 205.1 | 13.6 | 62.1 | 26.0 | 82.3 | 4.24 | 274.8 |
| Max | 18.50 | 1768.0 | 1131.5 | 7.79 | 7.6 | 80.0 | 50.4 | 191.9 | 5.1 | 389.2 | 30.5 | 93.8 | 36.0 | 367.1 | 5.90 | 382.6 |
| Min | 16.20 | 806.0 | 515.8 | 6.91 | 6.3 | 16.0 | 24.0 | 55.5 | 0.4 | 152.3 | 7.6 | 26.3 | 12.0 | 0.0 | 2.90 | 138.8 |

*3.2. Hydrochemical Modeling*

3.2.1. Hydrochemical Facies Using Piper Diagram

Piper's diagram helped to understand the geochemical evolution of GW sample and SW and its relationship with dissolved ions [102]. To better interpret the chemical composition of the GW sample [103–106] and the SW [12,107,108], anions were plotted on the right triangle while cations were plotted on the left [109]. The geochemical evolution of water in general (and GW in particular) can be assessed by determining chemical facies using Piper's trilinear diagram (1944) [110]. In the present study, Piper trilinear diagrams were plotted using scientific software called "Diagrammes".

Figure 4 shows that all samples fall in zone D (sodium-potassium cation facies type) with no magnesium or calcium types found on the cation side and zone G (chloride facies type) with no bicarbonate and sulfate types found on the anions side. Thus, the chemical composition of GW samples in the study area is dominated by strong acids ($Cl^-$) and alkalis ($Na^+$, $K^+$). According to the diamond diagram, all the samples were found in zone I (chloride, calcium sulfate, and magnesium) and II (sodium and potassium chloride). Essentially, the majority of the samples were characterized by the dominance of ($Na^+$, $K^+$), $Cl^-$, and $SO_4^{2-}$, and the Piper diagram revealed two types of water. As a result, the GW present facies of the sodium chloride to magnesium carbonate type, while SW are of the sodium chloride to magnesium sulfate type.

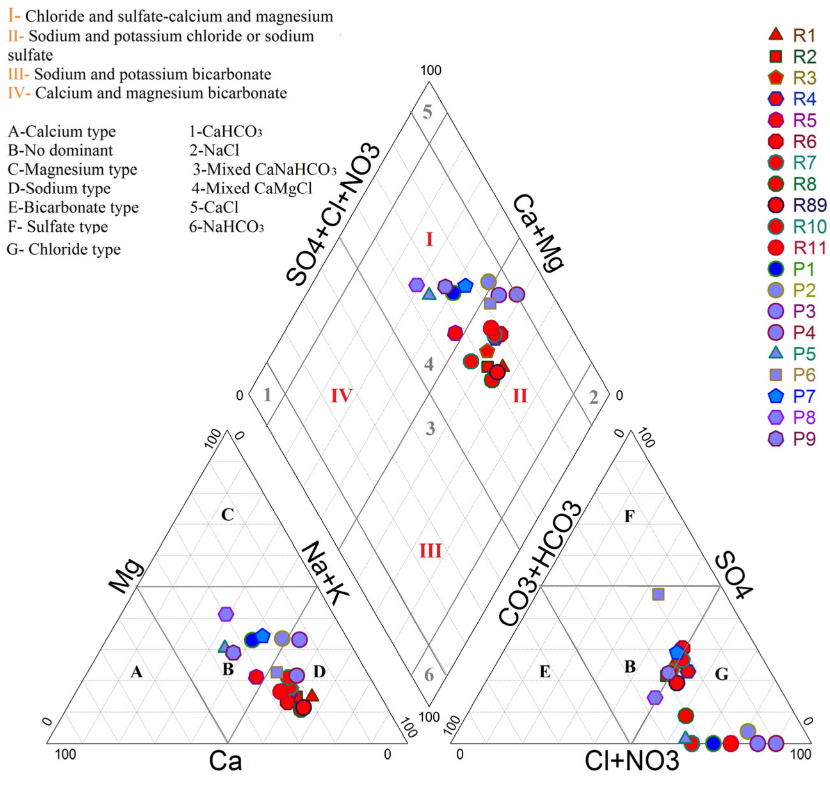


**Figure 4.** Chemical facies of GW–SW of the study area (Piper diagram).

Piper's diagram suggests that 77.77% of the GW samples (7 GW samples) belong to $Ca^{2+}$-$Mg^{2+}$-$Cl^-$-$SO_4^{2-}$ (field I), demonstrating the dominance of alkaline earths over alkali ($Ca^{2+} + Mg^{2+} > Na^+ + K^+$) and strong acidic anions over weak acidic anions (i.e., $Cl^- + SO_4^{2-} > HCO_3^-$), while all SW samples belong to $Na^+$, $K^+$, $Cl^-$ or $Na^+$ and $SO_4^{2-}$ which are plotted in File II, while 13 samples fell in zone D, indicating the dominance of sodium types (11 SW and P3, P6 in GW samples) [111].

3.2.2. Water Samples Schöeller Berkaloff Diagram and Schöeller Berkaloff Diagram for Average Parameters

The chemical composition of the GW from the Jouamaa Hakama site and the SW from the Ouljat Echatt river sampled has been represented on the Schöeller Berkaloff diagram [105,112] (Figure 5). The Schöeller Berkaloff diagram for the mean of the parameters reveals that the GW and SW parameters have the same pace and that the parameters progress proportionally in the same direction, except for $Mg^{2+}$ which progresses inversely proportional between GW and SW [113]. The average anion concentrations ($SO_4^{2-}$, $Cl^-$, and $HCO_3^-$) have been plotted on the right side of the figure while the average cation concentrations ($Ca^{2+}$, $Mg^{2+}$, $Na^+$, and $K^+$) were plotted on the left side of the Figure 5. The Schöeller Berkaloff diagram reveals that the $Ca^{2+}$ concentrations exceeded the concentrations of the other cations while the $Cl^-$ concentrations exceeded the concentrations of the other anions. The major ions in relative abundance are in the order $Ca^{2+} > Mg^{2+} > Na^+ > K^+$ for cations and $Cl^- > HCO_3^- > SO_4^{2-}$ for anions.

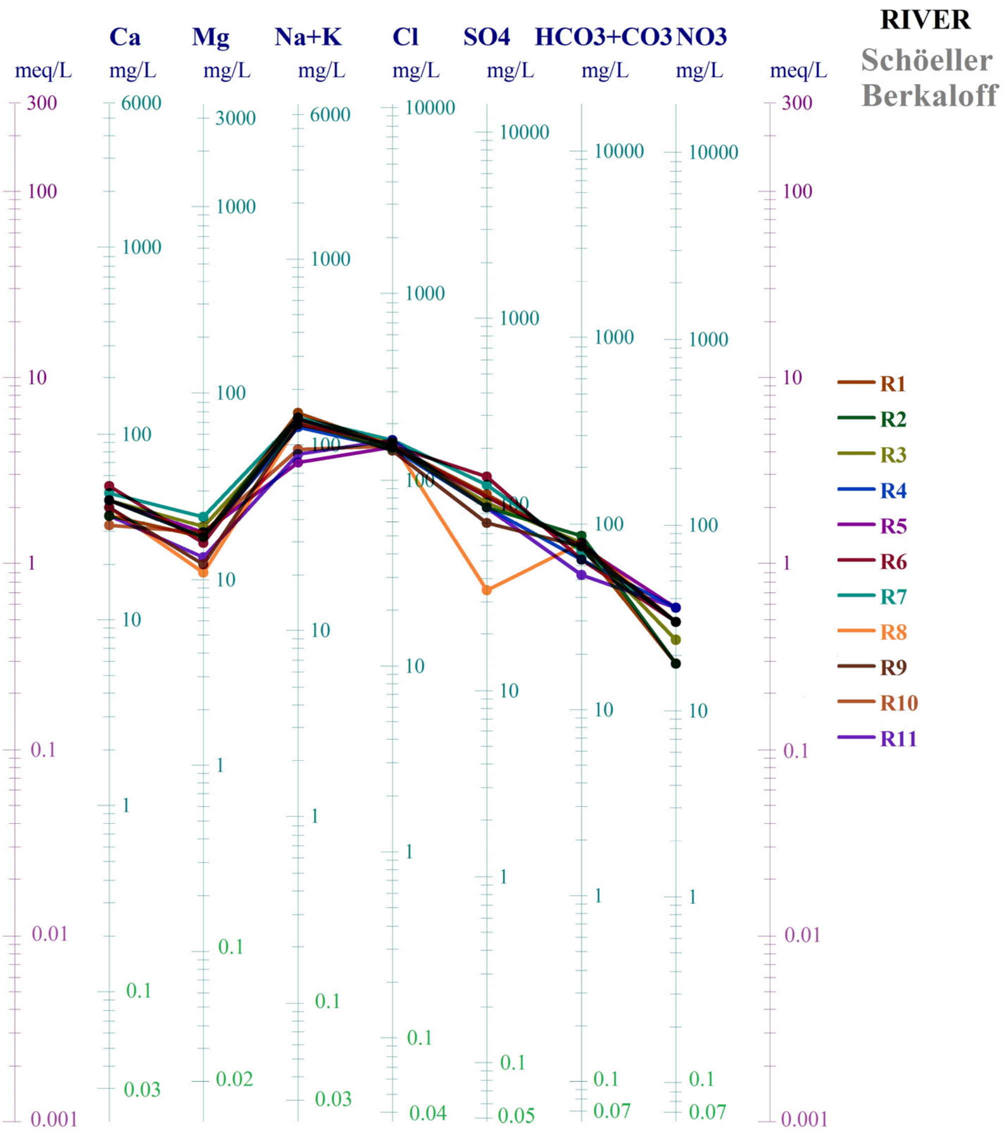


(**a**)

**Figure 5.** *Cont.*

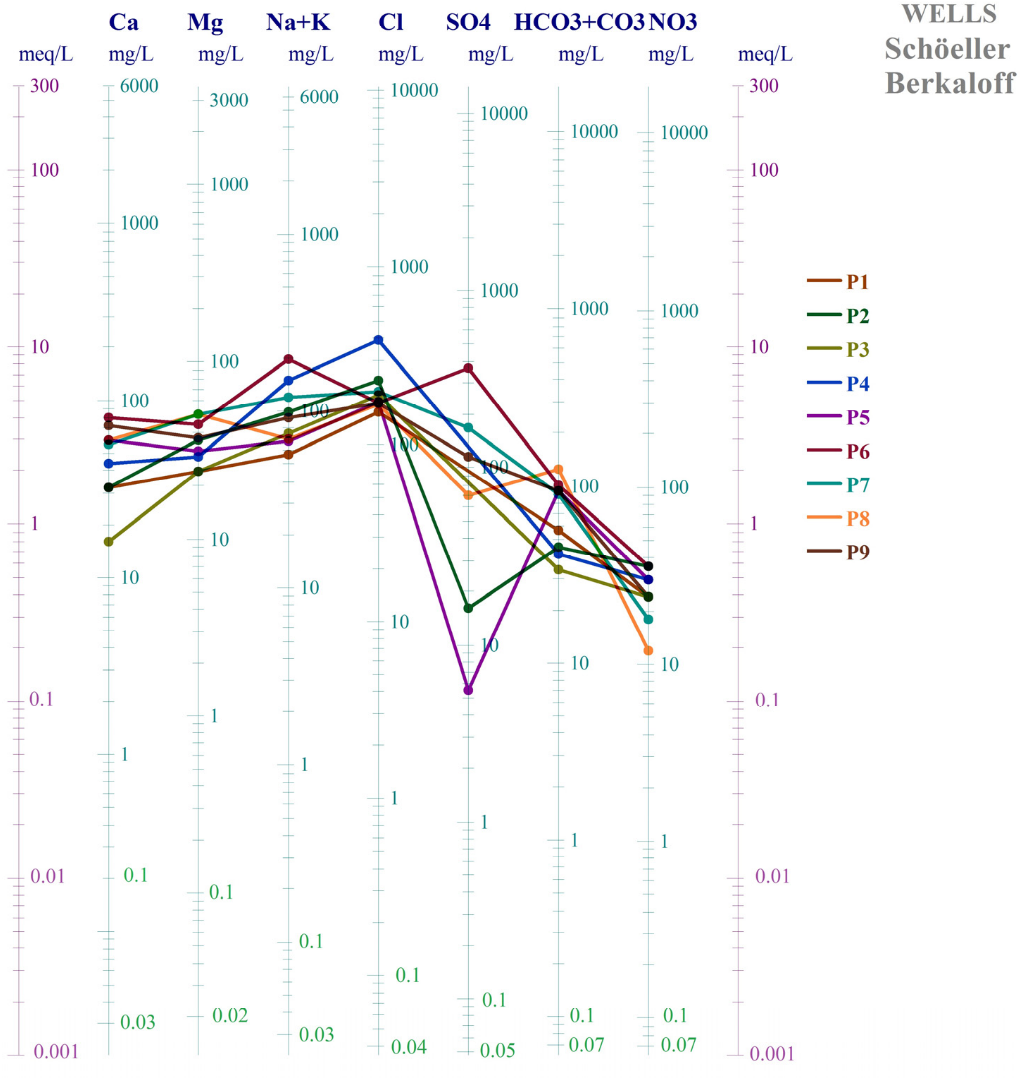


(**b**)

**Figure 5.** Water samples Schöeller Berkaloff diagram for river (**a**) and wells (**b**).

### *3.3. Groundwater Quality Index (GWQI) and Surface Water Quality Index (SWQI)*

The assessment of SW/GW quality was provided using the WQI, which presents a comprehensive picture of the water quality [114], because it categorizes water based on pollution levels into four groups [115].

Figure 6 shows that the WQI ranged from 55.60 to 208.22, indicating that the overall water quality of the river samples represented a value greater than 100 (unsuitable quality) (Table 7).

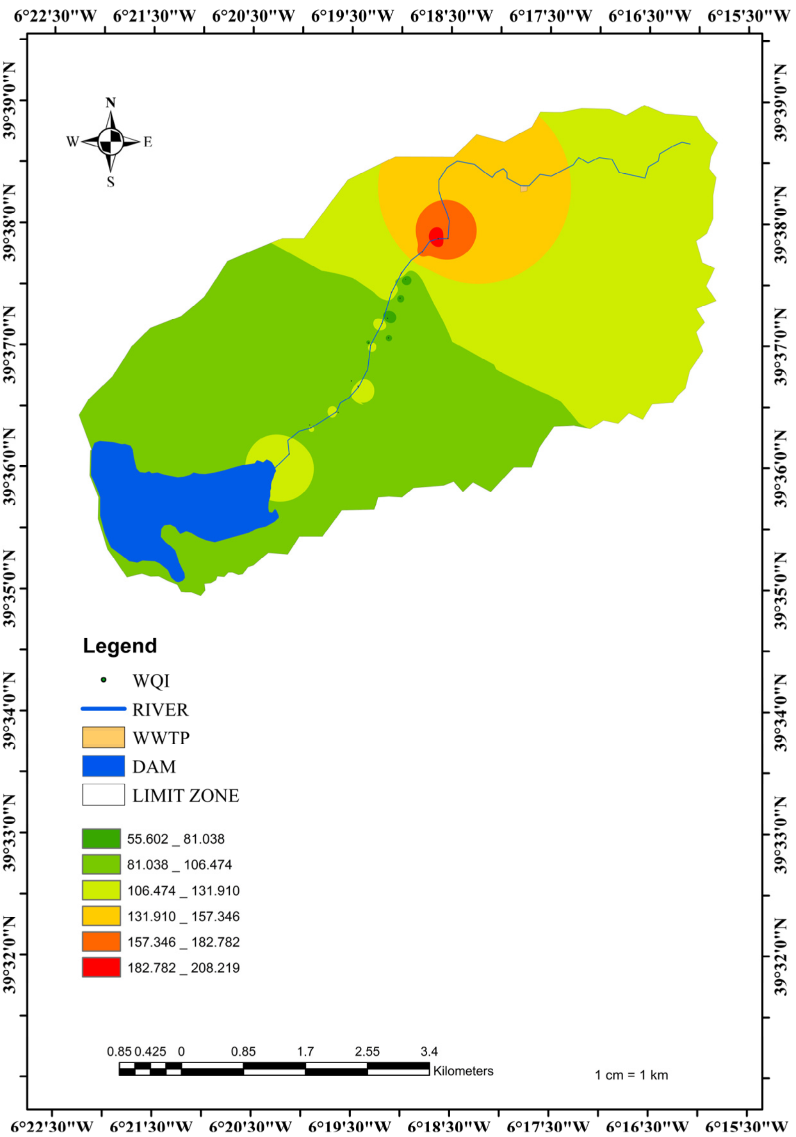


**Figure 6.** Spatial distribution of WQI.

**Table 7.** Classification GW and SW samples based on WQI.

| Samples River | WQI Score | Classification | Samples Wells | WQI Score | Classification |
|---|---|---|---|---|---|
| R1 | 165.497266 | Unsuitable | P1 | 59.6085173 | Poor |
| R2 | 208.221093 | Unsuitable | P2 | 74.295544 | Poor |
| R3 | 160.598102 | Unsuitable | P3 | 55.5992429 | Poor |
| R4 | 134.61429 | Unsuitable | P4 | 78.246694 | Very poor |
| R5 | 133.754536 | Unsuitable | P5 | 67.5059323 | Poor |
| R6 | 132.447409 | Unsuitable | P6 | 102.009686 | Unsuitable |
| R7 | 130.996801 | Unsuitable | P7 | 87.2619479 | Very poor |
| R8 | 124.981967 | Unsuitable | P8 | 88.2725732 | Very poor |
| R9 | 120.361114 | Unsuitable | P9 | 90.8769462 | Very poor |
| R10 | 111.714051 | Unsuitable | | | |
| R11 | 112.648884 | Unsuitable | | | |

Whereas all the river samples in R1, R3, R4, R5, R6, R7, R9, R10 and, R11 fell into the unsuitable quality category, the same was observed for P6. The highest value of 208.22 was recorded in the sample (R2), falling in class 4, which represents very poor water quality and requires special attention before use due to high levels of $Na^+$, $K^+$, and $CO_3^{2-}$.

The WQI indicated that 88.89% of the GW samples were poor for drinking (Figure 6). Compared to previous studies of WQI, we discovered similar results for surface water with new study in the north of Morocco [12], which reported that the WQI values of the Oued Laou River ranged between 9.01 and 149.27, indicating that the overall water quality of the studied river was graded from excellent to very poor. while in Tumkur Taluk, Karnataka State, India [116], the results indicated that the WQI of GW for these samples ranged from 89.21 to 660.56.

### *3.4. Irrigation Groundwater Water Quality (IGWQI) and Irrigation Water Quality of Surface Water (ISWQI)*

The EC values indicated by salinity damage are essential to evaluating the irrigation water [90]. Based on SAR values for the study area, most of the samples fell in the high or very high salinity (EC) category, and thus, most of the GW and SW can be classified as "doubtful" for irrigation, ranging from values of 750 to 2250 µS/cm. This is consistent with Richards' value, which indicated a doubtful water quality for irrigation according to the EC value (Table 8).

**Table 8.** Water quality parameters for irrigation in study area water samples.

| Samples | SAR | RSC | Na% | PI | KI | PS | RSBC | MH |
|---|---|---|---|---|---|---|---|---|
| R1 | 6..59 | −0.83 | 66.00 | 68.69 | 1.84 | 5.56 | −1.68 | 43.75 |
| R2 | 5.80 | −0.85 | 61.73 | 64.34 | 1.53 | 5.35 | −2.08 | 38.89 |
| R3 | 5.34 | −1.30 | 59.04 | 61.72 | 1.37 | 5.32 | −2.08 | 42.11 |
| R4 | 5.26 | −1.60 | 59.27 | 62.20 | 1.39 | 5.23 | −2.08 | 38.89 |
| R5 | 3.22 | −1.33 | 47.43 | 50.76 | 0.84 | 4.27 | −2.08 | 40.54 |
| R6 | 5.66 | −1.90 | 60.02 | 62.63 | 1.43 | 5.79 | −2.48 | 33.33 |
| R7 | 5.50 | −1.95 | 58.40 | 60.88 | 1.34 | 6.01 | −2.28 | 42.86 |
| R8 | 6.01 | −0.40 | 65.03 | 68.24 | 1.76 | 4.93 | −1.88 | 31.03 |
| R9 | 6.21 | −0.63 | 65.34 | 68.40 | 1.79 | 4.96 | −1.88 | 33.33 |
| R10 | 4.30 | −0.73 | 56.22 | 60.10 | 1.22 | 4.36 | −1.48 | 48.39 |
| R11 | 4.19 | −1.40 | 56.47 | 62.90 | 1.23 | 4.70 | −1.55 | 37.93 |
| P1 | 2.54 | −1.85 | 40.30 | 46.00 | 0.67 | 4.35 | −1.48 | 55.56 |
| P2 | 4.01 | −3.23 | 48.37 | 52.29 | 0.93 | 6.77 | −1.48 | 65.22 |
| P3 | 3.75 | −1.80 | 53.29 | 58.81 | 1.12 | 5.41 | −0.68 | 71.43 |
| P4 | 5.93 | −3.35 | 58.26 | 61.27 | 1.38 | 11.12 | −2.08 | 52.17 |
| P5 | 2.40 | −2.73 | 33.97 | 39.56 | 0.51 | 5.05 | −2.75 | 46.43 |
| P6 | 6.01 | −4.70 | 52.34 | 55.82 | 1.08 | 8.73 | −3.63 | 48.05 |
| P7 | 3.87 | −4.25 | 42.50 | 46.36 | 0.73 | 7.38 | −2.55 | 60.00 |
| P8 | 2.08 | −3.58 | 28.89 | 35.04 | 0.39 | 5.57 | −2.50 | 58.33 |
| P9 | 3.02 | −3.70 | 37.11 | 40.20 | 0.58 | 6.07 | −3.48 | 46.27 |

SAR is used to categorize SW and GW into four groups: "Excellent" ($SAR < 10$); "Good" ($10 < SAR < 18$); "Suspicious" ($18 < SAR < 26$); and "Unsuitable" ($SAR > 26$). Water sample SAR varied from 2.08 to 6.59 (Table 8). As a result, according to a USSL diagram, the categorization of irrigation water quality is in the form of EC against SAR values. EC is used as the salinity risk index and SAR gives the sodium risk for irrigation water. According to the Richards classification [93], the plot revealed that about 100% of the SW and GW samples fell into the C3-S1 category, which shows that the SW in the investigated area had a medium salinity and low sodium content (Figure 7). The SW in the study area was within a low salinity field (<2250 µS/cm), thus the water is highly appropriate for irrigation and the SAR class (S1). These findings are in alignment with the Wilcox diagram in Figure 8.

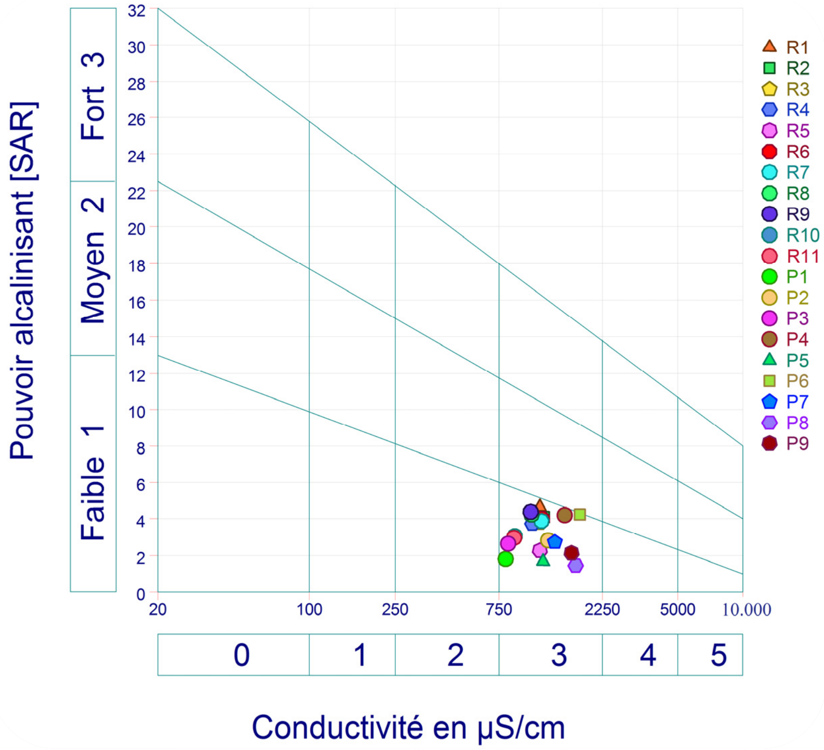


**Figure 7.** Riverside diagram for GW and river water.

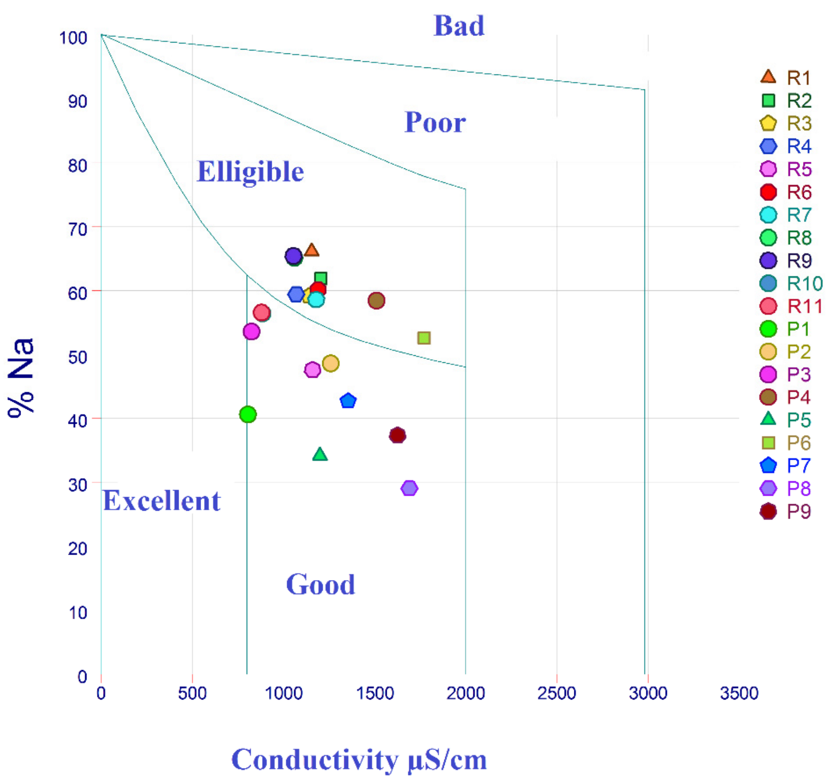


**Figure 8.** Wilcox diagram for GW and river water.

According to Table 8, the Na% in irrigation water samples ranged from 28.89% to 66%, with an average of 52.50%. As a result, the Wilcox plot for percent of sodium and total concentration displayed in Figure 8 indicates that 50% of the water samples (7 GW and 3 SW samples) were in good condition, while 50% were "eligible" with excessive content (2 GW and 8 SW samples).

The magnesium hazard (MH) parameter was proposed by Paliwal et al. [98]. The MH values varied from 31.03 to 71.43%, but only 33.33% of the water samples had a value of less than 50 for well samples. Fully 100% of SW was considered suitable for irrigation. However, 66.77% of GW had a MH greater than 50.

Sodium calculated against $Ca^{2+}$ and $Mg^{2+}$ was considered by the Kelley index (KI) [96]. Kelly's ratio (KI > 1) indicates an excess level of sodium in water that is unsuitable for irrigation, while KI less than 1 is suitable for irrigation uses. According to Kelly's ratio, the samples varied from 0.39 to 1.84 meq/L, which means the majority of samples were non-permissible (65%), and just 35% were suitable for irrigation purposes. The GW in six samples and one sample of SW (R5) was deemed adequate for irrigation [117].

The PI, developed by Doneen et al. [95], can better reflect the effects of irrigation, (Table 8). It spanned from 35.04% to 68.40%. Nearly 100% of the samples (SW and GW) fell under the Class II category, indicating that the water was moderately too good for irrigation purposes.

From the results, the RSC values ranged from −4.70 to −0.40 meq/L (Table 8). These values are lower than 1.25 meq/L, which corresponds to the "safe/good" category according to the classification.

The residual sodium bicarbonate index (RSBC) is used to determine the risk of alkalinity and was proposed by Gupta et al. who classified RSBC into two categories and found that RSBC values above 10.0 meq/L affected plant growth in several ways, while RSBC values below 5 meq/L were considered satisfactory [97]. In this study, the findings indicate that RSBC values varied from −3.63 to −0.68 meq/L (Table 7), indicating that all samples had RSBC values well below the acceptable level and could be safely used for irrigation.

One of the classifications used to assess the suitability of water for irrigation is potential salinity (PS), which is the concentration of $Cl^{-}$ added to half the concentration of $SO_4^{2-}$. Among the samples examined, the potential salinity varied between 4.27 meq/L and 11.12 meq/L (Table 8). This indicates that 11.11% of the wells (P1) and 45.45% of the surface waters (R5, R8, R9, R10, and R11) are classified as "good" while 54.55% and 88.89% of the surface and well samples are classified as "unsuitable" for irrigation (Table 8) [95].

### *3.5. Multivariate Statistical Analysis*

#### 3.5.1. Statistical Analysis (PCA)

Table 9 explains 83.58% of the data's overall variance. The F1–F2 combination represents more than 64.91% of the data (Figure 9). The first component (F1) represented 41.73% of the total variation, with significant positive loadings of EC, TDS, $Ca^{2+}$, $Mg^{2+}$, and TH and moderate loadings of pH and $HCO_3^{-}$. This component indicates that EC in SW is influenced by the amounts of TDS, $Ca^{2+}$, and $Mg^{2+}$. This component's substantial $Ca^{2+}$ loading may explain why $Ca^{2+}$ predominates in SW samples over $Mg^{2+}$. This component is generally associated with anthropogenic contamination. The presence of $Mg^{2+}$ ions in the research area suggests that they were formed as a result of interactions between the dolomitic limestone and water.

**Table 9.** Correlation between the physical and chemical parameters.

| Variables | T | EC | TDS | pH | DO | Ca | Mg | Na | K | Cl | $HCO_3$ | $CO_3$ | $NO_3$ | $SO_4$ | TH |
|---|---|---|---|---|---|---|---|---|---|---|---|---|---|---|---|
| T | **1** | | | | | | | | | | | | | | |
| EC | −0.224 | **1** | | | | | | | | | | | | | |
| TDS | −0.224 | **1.000** | **1** | | | | | | | | | | | | |
| pH | −0.327 | **0.566** | **0.566** | **1** | | | | | | | | | | | |
| DO | **−0.721** | −0.069 | −0.069 | 0.198 | **1** | | | | | | | | | | |
| Ca | 0.001 | **0.834** | **0.834** | **0.520** | −0.236 | **1** | | | | | | | | | |
| Mg | **−0.476** | **0.729** | **0.729** | **0.652** | 0.327 | **0.578** | **1** | | | | | | | | |
| Na | 0.136 | 0.427 | 0.427 | 0.083 | −0.176 | 0.360 | 0.002 | **1** | | | | | | | |
| K | **0.605** | −0.242 | −0.242 | **−0.450** | **−0.596** | −0.133 | **−0.690** | 0.344 | **1** | | | | | | |
| Cl | −0.406 | 0.335 | 0.335 | 0.435 | 0.254 | −0.029 | 0.297 | 0.217 | **−0.484** | **1** | | | | | |
| $HCO_3$ | −0.043 | **0.567** | **0.567** | **0.495** | −0.078 | **0.553** | **0.685** | −0.026 | −0.258 | −0.030 | **1** | | | | |
| $CO_3$ | 0.132 | **0.519** | **0.519** | 0.318 | −0.387 | **0.703** | 0.322 | 0.091 | 0.236 | **−0.451** | 0.435 | **1** | | | |
| $NO_3$ | 0.367 | −0.185 | −0.185 | **−0.450** | −0.172 | −0.046 | −0.332 | 0.163 | 0.011 | 0.085 | −0.259 | −0.419 | **1** | | |
| $SO_4$ | 0.071 | **0.593** | **0.593** | 0.217 | −0.101 | **0.694** | 0.382 | **0.747** | 0.144 | −0.194 | 0.366 | **0.453** | −0.044 | **1** | |
| TH | −0.310 | **0.867** | **0.867** | **0.670** | 0.102 | **0.847** | **0.924** | 0.171 | **−0.512** | 0.180 | **0.706** | **0.541** | −0.238 | **0.575** | **1** |

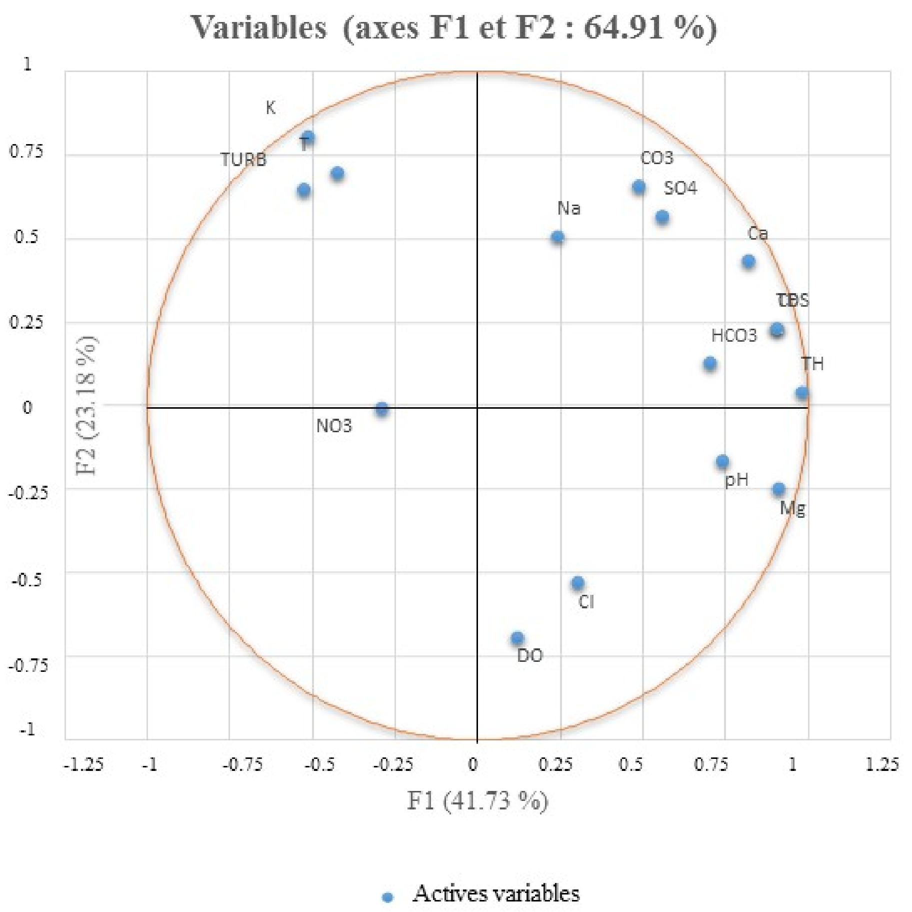


**Figure 9.** Parameters correlation of GW–SW quality based on PCA.

The presence of $CO_3{}^{2-}$ and $HCO_3{}^{-}$ in this component suggests that SW alkalinity is related to bicarbonate ions, which is the result of a natural disintegration process of the calcareous sedimentary rocks and anthropogenic. The $HCO_3{}^{-}$ has a moderate loading on the F1 factor, indicating that it was formed through weathering, carbonate dissolution, and bacterial decomposition of organic pollution, among other processes [12]. Stations R4, R5, R8, R9, R10, R11, P6, P7, P8, and P9 also had the greatest impact on the F1 score.

With moderate positive loadings of T, $CO_3^{2-}$, $K^+$, $SO_4^{2-}$, and TURB, the second component (F2) explains 23.179% of the overall variance, although $SO_4^{2-}$ is primarily derived from soluble inorganic nitrogen and inorganic salts. Additionally, this important T value is due to the depth of the wells. Stations P1, P2, P3, R3, R6, and R7 had the greatest influence on the F2 score. F3 accounts for 11.041% of total variability and is distinguished by significant positive $Na^+$ and $Cl^-$ loading. The presence of $Na^+$ in this component suggests that the primary ions at the research site regulate surface water mineralization. This is what we noticed in station P4, which accounted for the majority of factor F3.

The fourth component (F4) indicates that $NO_3^-$ with a moderate load caused 7.628% of the total variance, which is mostly associated with the use of fertilizers and wastewater, while the significant positive loading of DO for this component could indicate a fluctuation of nitrates in surface waters. Stations R1, R2, and P5 accounted for the majority of F4 scores. The positive charge for factors 1 and 2 is more important than for 3 and 4. This indicates that they are the result of rock–water interaction in the GW–SW interaction and that anthropogenic activities can have a considerable impact.

#### 3.5.2. Pearson's Coefficient of Correlation (r)

Based on the analysis of the Pearson correlation matrix in Table 9, the significant correlation coefficient between EC and TDS suggests that water conductivity depends on TDS, while EC and TDS had positive correlations with $Ca^{2+}$, $Mg^{2+}$, pH, $Cl^-$, $HCO_3^-$, $CO_3^{2-}$, TH, and $SO_4^{2-}$ which gives information about salinity and mineralization of GW and SW [118,119].

A moderate correlation ($r > 0.5$) was observed between $Ca^{2+}$ and $Mg^{2+}$, indicating that water TH is defined as the combined concentration of calcium and magnesium ions in water samples. SW was high in $Na^+$, $NO_3^-$, $Cl^-$ and $SO_4^{2-}$. pH is moderately correlated with EC, TDS, TH, $HCO_3^-$, $NO_3^-$, and $Cl^-$ (but negatively correlated with $K^+$ ($r = -0.450$), indicating that pH affects the release or dissolution of $K^+$, $Na^+$, $NO_3^-$, and $Cl^-$ in solution. There was also a significant positive correlation ($r = 0.703$) between $Ca^{2+}$ and ($HCO_3^-$ and $CO_3^{2-}$), indicating the geogenic origin of GW contamination. Furthermore, there is a strong correlation between $Ca^{2+}$ and $SO_4^{2-}$, indicating that common sources are the primary source of GW pollution, especially in our area which is close to industrial activities. There was a strong positive correlation among $Mg^{2+}$, $Ca^{2+}$, and TH; on the other hand, a negative correlation was observed between $Mg^{2+}$ and $K^+$. This implies that these cations possibly originate from the same source.

In addition, a strong correlation was observed between $Na^+$ and $SO_4^{2-}$. The association of $HCO_3^-$ and $Mg^{2+}$, as well as an additional source of $CO_3^{2-}$ most likely resulting from the dissolution of calcite. It is thought that dolomite enriches GW with $Mg^{2+}$, $HCO_3^-$, and $CO_3^{2-}$. The authors of [120,121] discovered comparable results regarding the correlation between $SO_4^{2-}$ and $K^+$. The pH showed a positive and significant correlation with $Ca^{2+}$ ($r = 0.509$), $Mg^{2+}$ ($r = 0.498$), and $HCO_3^-$ ($r = 0.529$). These correlation results indicated mixed sources of either geogenic or anthropogenic origin.

### *3.6. Distribution of the Main Ion Concentrations according to the Distance from the River*

The interaction between SW and GW samples was compared using linear regression of the samples from the wells and the river two by two along the segment of the river downstream of the WWTP, which gave a significant coefficient of determination, $R^2 = 85.6\%$. (Figure 10). Logarithmic regression was also established based on the observation of hydrochemical parameters to investigate the interactions between SW and GW by comparing the concentration of each parameter moving away from the riverbed towards the wells in a band of 100 m on either side of the river, which showed different $R^2$ values ranging from 50% to 83% along the river (Figure 11).

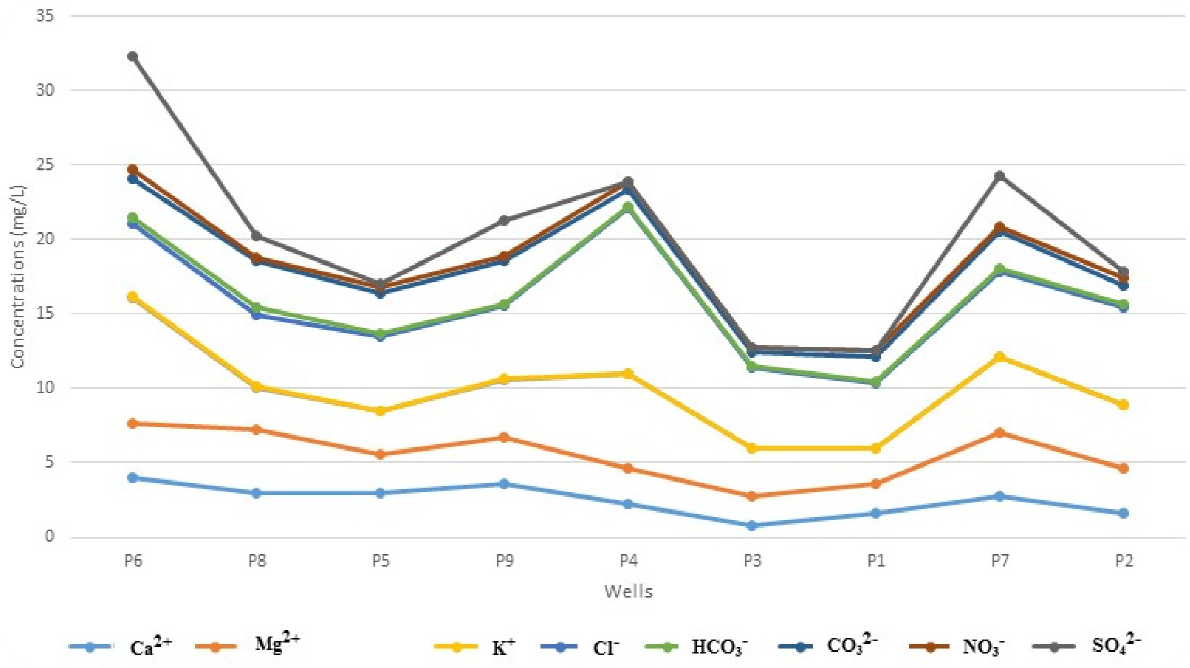


**Figure 10.** Spatial variations of major ion concentrations in river water.

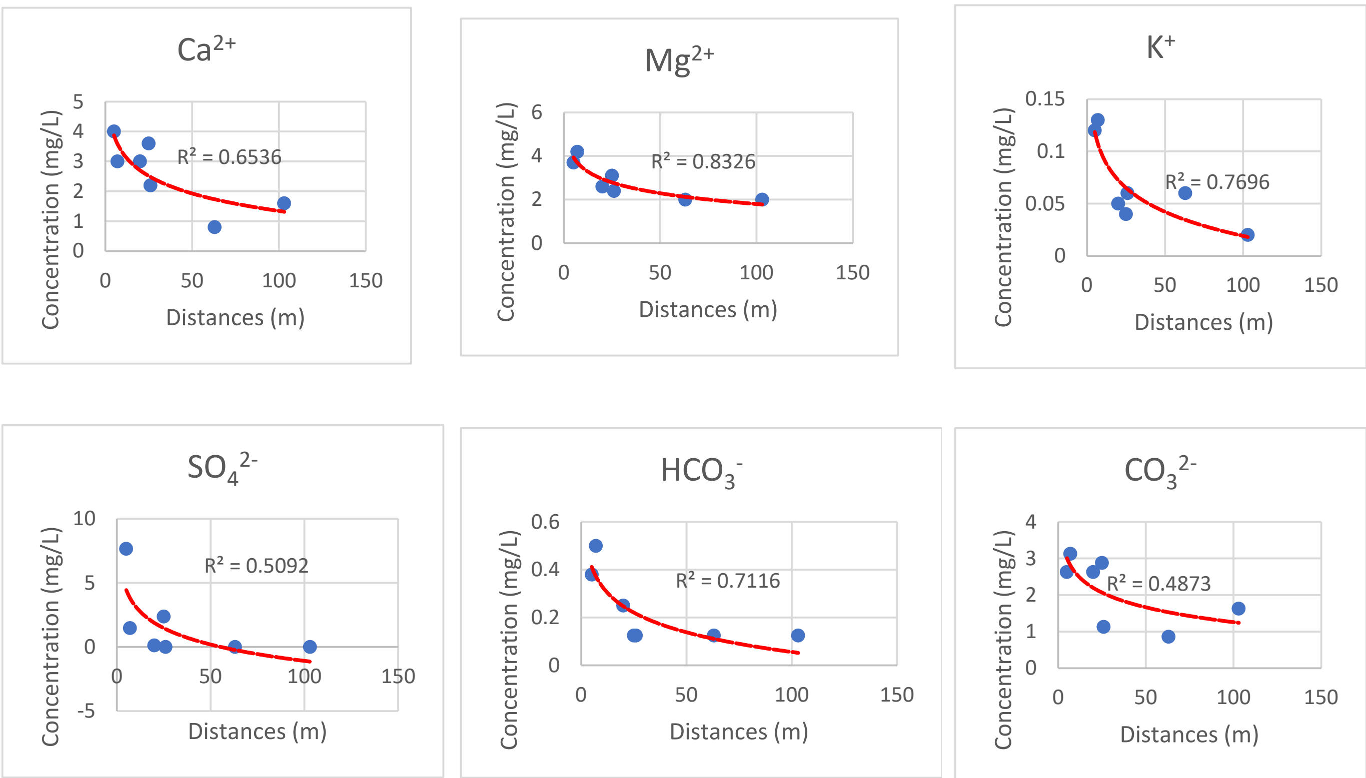


**Figure 11.** *Cont.*

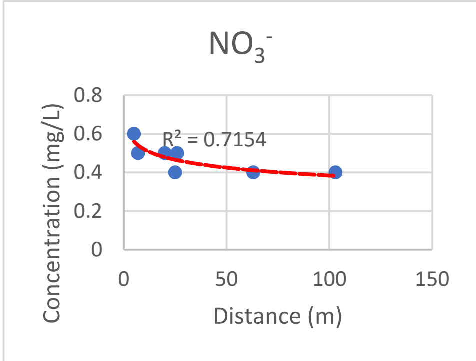


**Figure 11.** Plots of major ion concentrations in groundwater vs. distance from river.

According to the logarithmic regression analysis, we can conclude that the wells near the river showed higher $R^2$ values (P6–P8) than those at a big distance (P3, P4). The IDW expressed as a transverse and longitudinal gradient and the higher logarithmic regression coefficients ($R^2 > 0.70$) of $Mg^{2+}$, $K^+$, $NO_3^-$, and $HCO_3^-$ indicate that SW and GW interact, which enables us to deduce clear information about the types of variables that impact the interaction (the distance between the river and well).

### 3.7. Interpretation for GW–SW Interactions with Hydrochemical Data

According to Figure 12, the hydrochemical parameters are positively correlated with a strong significance ($R^2 = 0.85$), which explains the interaction between the GW of the Jouamaa Hakama site and the SW of the Ouljat Echatt River. In addition, interpolation (IDW) of the different parameters analyzed in this study shows a cross-gradient (transverse gradient) between GW and SW (Figure 13), which explains the GW–SW connection along the 100 m strip on both sides of the river downstream WWTP discharges. We can note that the intensity and significant concentrations of the parameters are high in the wells that are near the river (Figure 11).

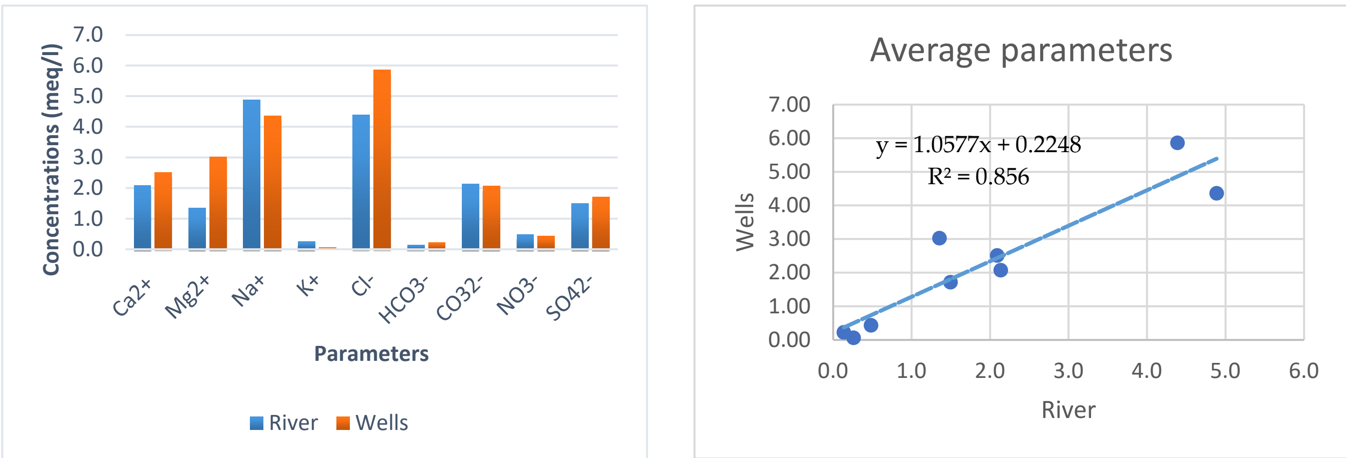


(**a**) (**b**)

**Figure 12.** (**a**) Ionic concentrations average in the GW and SW. (**b**) Correlation between Ionic concentrations average in GW and SW.

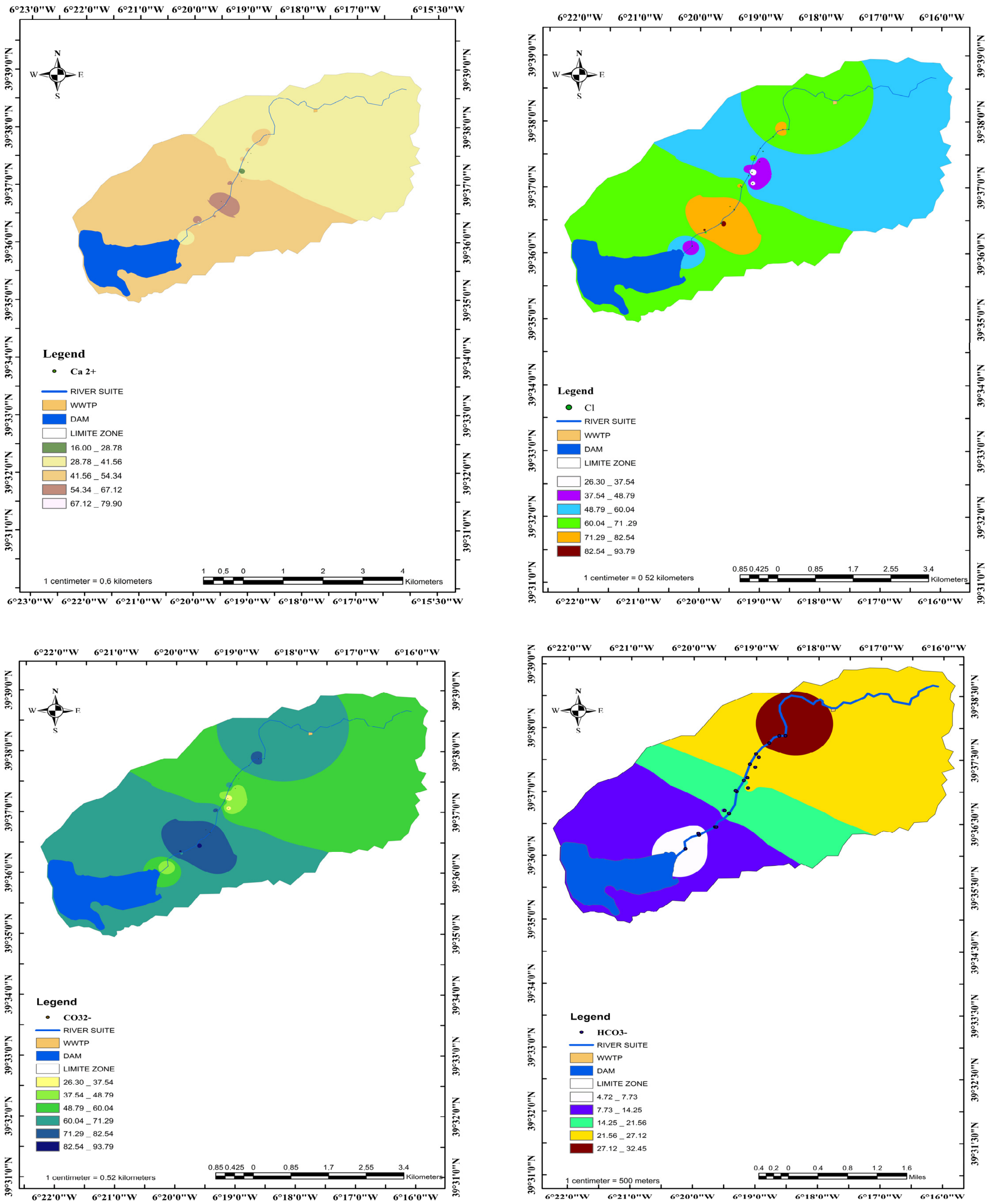


**Figure 13.** *Cont.*

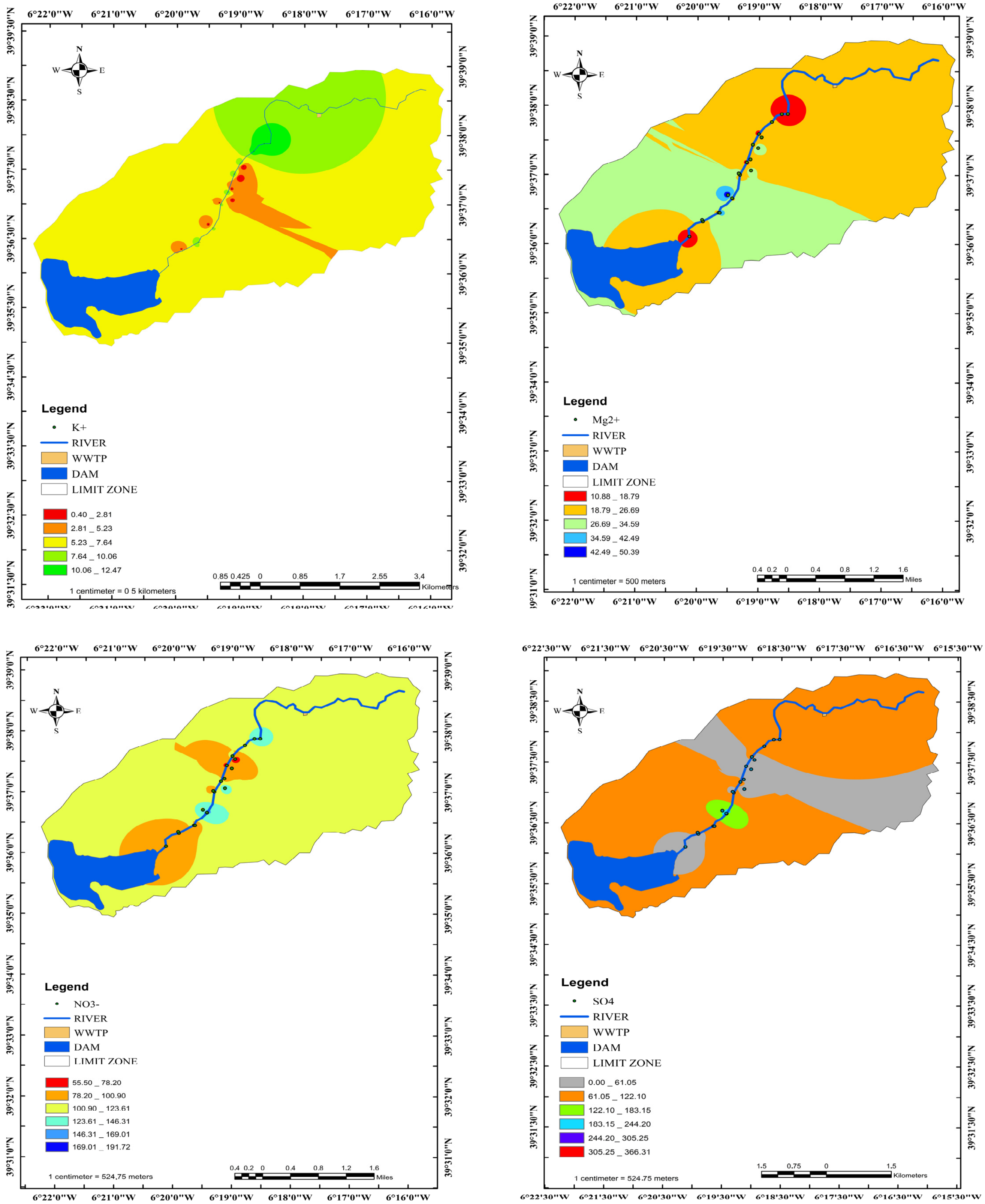


**Figure 13.** *Cont.*

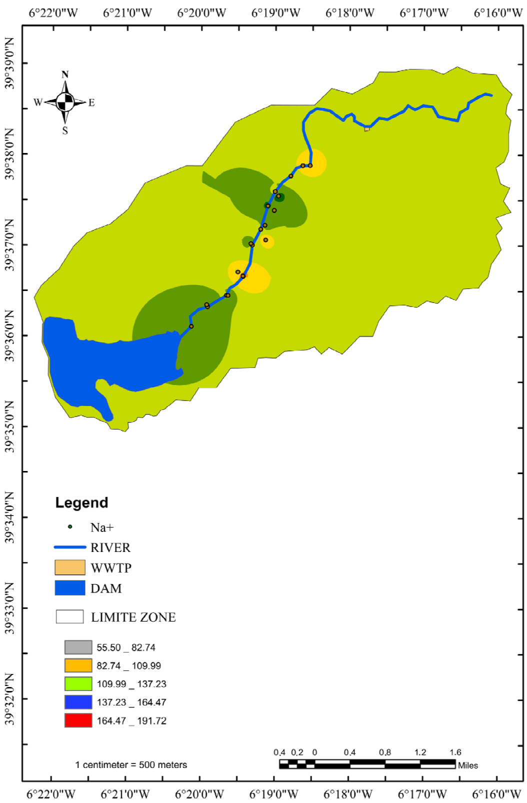


**Figure 13.** Spatial distribution map of GW and SW for cations and anions.

The similarity in the concentration of the majority of freshwater hydrochemical parameters in the river basin demonstrated the hydrological connectivity between GW and SW on the strip at a distance of 100 m left and right of the river. According to WQI, the GW in the GW–SW connection band was evaluated as having poor to very poor qualities in all wells. We report that the well number 6 closest to the river is of unsuitable quality for consumption. Additionally, the WQI of the different sampling points of the river is all of unsuitable quality.

## 4. Conclusions

Water stress, pollution by various anthropogenic activities, and climate change are current issues. These changes affect the quality of the water, which has negative effects on human health and the environment. In Morocco, a large number of people use the inland water for drinking and other purposes in both urban and rural areas. For that reason, this study aims to assess and identify the interaction between SW and GW to assess the sources of surface water pollution from the downstream discharges from the WWTP treated effluents from the TAC industrial zone in northern Morocco and determine the interference of polluted SW with shallow aquifer waters. This situation will require control and permanent monitoring because it is a major hydric resource management problem.

Freshwater hydrochemistry was examined to identify interactions between the Ouljat Echatt River SW and GW of the Jouamaa Hakama site. Spatial analysis of hydrochemical data of well water (9 well water samples) and Ouljat Echatt river water (11 SW samples) was done using hydrochemical methods, WQI and IWQI, multivariate statistics, and GIS-based Inverse Distance Weighted Interpolation. A total of 16 physicochemical parameters were analyzed, and an assessment of the surface water adequacy of irrigation was carried out. This study examined freshwater hydrochemistry to identify interactions between the Ouljat Echatt River SW and GW of the Jouamaa Hakama site. The work was carried out downstream of the discharges from the WWTP treated effluents from the TAC industrial zone in northern Morocco. Spatial analysis of hydrochemical data of well water (nine well water samples) and Ouljat Echatt river water (eleven SW samples) was undertaken using a methodology based on hydrochemical modeling (HM) and PCA, WQI, irrigation indices, GIS-based Inverse Distance Weighted Interpolation, and regression analysis.

The results indicated that the major ions found in GW and SW were characterized in a different order in the anion list order $Cl^- > CO_3^{2-} > NO_3^- > HCO_3^- > SO_4^{2-}$ and $Cl^- > SO_4^{2-} > CO_3^{2-} > NO_3^- > HCO_3^-$, respectively, while the concentrations of cations showed the same order for both: $Na^+ > Ca^{2+} > Mg^{2+} > K^+$. As a result, GW showed in the Piper diagram as the sodium chloride to magnesium carbonate type, while SW belonged to the sodium chloride to magnesium sulfate type.

According to the WQI calculated, the total well samples were rated as poor and very poor. In addition, the calculated SWQI was rated as unsuitable for the total river samples. The hydrochemical and statistical results suggest that there is an interaction between SW and GW along the river segment downstream from the industrial area. We report that well number 6, near the river, is unsafe for human consumption. Furthermore, the WQI of the river's many sample stations is all of poor quality. Based on the results of hydrochemical parameters, we found a positive correlation with a strong significance ($R^2$ = 0.85) that explains the interaction between the GW of the Jouamaa Hakama site and the SW of the Ouljat Echatt River. In addition, interpolation (IDW) of the different parameters analyzed in this study shows a transverse gradient between GW and SW, which explains the GW–SW connection along the 100 m strip on both sides of the river. We can also remark that the intensity and significant concentrations of the parameters are high in the wells that are near the river. According to the logarithmic regression analysis, we can conclude that the wells near the river showed higher $R^2$ values (P6–P8) than those at a big distance (P3, P4). The IDW expressed as a transverse and longitudinal gradient and the higher logarithmic regression coefficients ($R^2 > 0.70$) of $Mg^{2+}$, $K^+$, $NO_3^-$, and $HCO_3^-$ indicate that SW and GW interact, which enables us to deduce clear information about the types of variables that impact the interaction (the distance between the river and well).

Through these results, the use of emerging techniques and mathematical models makes it possible to characterize the quality of land waters and shows the importance of an approach combining hydrochemical data interpreted by multivariate statistics and GIS techniques for the assessment of GW–SW interaction in downstream treated discharges from the TAC industrial zone in northern Morocco. Accordingly, policymakers and water managers in Morocco can use the results derived from a new coupled framework to achieve sustainable GW and SW management, prevent anthropogenic activities nationwide, and consolidate bases of sustainable development. This technique is intended to provide an accurate representation of the interaction between SW and GW; this is why it is highly recommended that it be applied to other studies with similar areas to monitor the state of water resources in Morocco. Other investigations, such as heavy metal analysis and bacteriological analysis, are required to fully understand the interaction of GW and SW as well as the influence of surface water on groundwater, which can be confirmed by repeat sampling.

If no measures are taken to limit river degradation, the pollution will eventually be diffused into the underground waters beyond the 100 m band studied. Basically, to prevent the contamination of groundwater by polluted surface water, it is necessary to use the process of bioremediation, which involves using plants to extract the contamination from surface water in the rhizosphere by using their roots. Additionally, digging wells farther from the river at a distance greater than 100 m can another solution, as well as using chlorine for water treatment and biological filters such as reeds.

**Author Contributions:** Conceptualization, E.M.A., E.K.C., F.S. and H.D.; methodology, E.M.A., H.E.A., E.K.C., H.Y., A.G. and N.N.; software, E.M.A., H.E.A., E.K.C., H.D. and N.N.; validation E.K.C., E.M.A., F.S. and H.D.; formal analysis, H.E.A., E.K.C., E.M.A. and F.S.; writing—original draft preparation, E.M.A., F.S., H.D. and H.E.A.; writing—review and editing, H.D., E.M.A., H.E.A., E.K.C., H.Y., A.G., N.N. and J.E.d.S.; visualization, E.K.C. and E.M.A.; supervision, E.K.C., J.E.d.S. and F.S.; funding acquisition, J.E.d.S. and E.K.C. All authors have read and agreed to the published version of the manuscript.

**Funding:** This research received no external funding.

**Data Availability Statement:** Not applicable.

**Acknowledgments:** This work was done within the framework of FCT ("Fundação para a Ciência e Tecnologia", Portugal) funded projects UIDB/00081/2020 (CIQUP) and LA/P/0056/2020 (IMS). The authors express their gratitude to INRA, CRRAR, URECRN, and Rabat for the invaluable help in carrying out this work and the support provided in the physicochemical analyses of the water samples.

**Conflicts of Interest:** The authors declare no conflict of interest.

## References


1. Dakkak, H.; Zouahri, A.; Iaaich, H.; Moussadek, R.; Elkhadir, M.; Douaik, A.; Soudi, B.; Benmohammadi, A. Apport Des Systèmes d'Information Géographique Au Diagnostic de La Pollution Nitrique Des Eaux Souterraines: Cas de La Zone de Skhirate–Maroc. Available online: https://www.researchgate.net/profile/Ahmed-Douaik/publication/262378124_Apport_des_Systemes_d\T1\textquoterightInformation_Geographique_au_diagnostic_de_la_pollution_nitrique_des_eaux_souterraines_Cas_de_la_zone_de_Skhirate_-_Maroc/links/5698970e08ae1c42790560a0/Apport-des-Systemes-dInformation-Geographique-au-diagnostic-de-la-pollution-nitrique-des-eaux-souterraines-Cas-de-la-zone-de-Skhirate-Maroc.pdf (accessed on 1 March 2023).
2. Hind, E.S. Vulnérabilité à La Pollution Des Eaux Souterraines: Aspects Dynamique et Application à l'aquifère de R'Mel (La-rache, Maroc). *Int. J. Innov. Appl. Stud.* **2015**, *6*, 929–940.
3. Belhadj, M.Z. Qualité Des Eaux de Surface et Leur Impact Sur l'environnement Dans La Wilaya de Skikda. Ph.D. Thesis, Université Mohamed Khider-Biskra, Biskra, Algeria, 2017.
4. Belhassan, K.; Hessane, M.A.; Essahlaoui, A. Interactions eaux de surface–eaux souterraines: Bassin versant de l'Oued Mikkes (Maroc). *Hydrol. Sci. J.* **2010**, *55*, 1371–1384. [CrossRef]
5. Wang, W.; Chen, Y.; Wang, W.; Zhu, C.; Chen, Y.; Liu, X.; Zhang, T. Water quality and interaction between groundwater and surface water impacted by agricultural activities in an oasis-desert region. *J. Hydrol.* **2023**, *617*, 128937. [CrossRef]
6. Ogwueleka, T.C.; Christopher, I.E. Hydrochemical interfaces and spatial assessment of Usuma River water quality in North-Central Nigeria. *Sci. Afr.* **2020**, *8*, e00371. [CrossRef]
7. Dawoud, M.A.; Raouf, A.R.A. Groundwater Exploration and Assessment in Rural Communities of Yobe State, Northern Nigeria. *Water Resour. Manag.* **2008**, *23*, 581–601. [CrossRef]
8. Tirkey, P.; Bhattacharya, T.; Chakraborty, S.; Baraik, S. Assessment of groundwater quality and associated health risks: A case study of Ranchi city, Jharkhand, India. *Groundw. Sustain. Dev.* **2017**, *5*, 85–100. [CrossRef]
9. Gulgundi, M.S.; Shetty, A. Groundwater quality assessment of urban Bengaluru using multivariate statistical techniques. *Appl. Water Sci.* **2018**, *8*, 43. [CrossRef]
10. Azzirgue, E.M.; Salmoun, F. Assessment of the Physico-Chemical Quality of Water of Oued Ouljat Echatt and Dam Ibn Batouta-Tangier. *Int. J. Adv. Sci. Res. Eng.* **2019**, *5*, 314–324. [CrossRef]
11. Azzirgue, E.M.; Farida, S.; El Khalil, C.; Mejjad, N. Determination of the Jouamaa Groundwater Quality Using Physi-co-Chemical Water Analysis and Geographic Information System. In *E3S Web of Conferences*; EDP Sciences: Les Ulis, France, 2021; Volume 314, p. 07006.
12. Azhari, H.E.; Cherif, E.K.; Sarti, O.; Azzirgue, E.M.; Dakak, H.; Yachou, H.; Esteves da Silva, J.C.; Salmoun, F. Assessment of Surface Water Quality Using the Water Quality Index (IWQ), Multivariate Statistical Analysis (MSA) and Geographic Infor-mation System (GIS) in Oued Laou Mediterranean Watershed, Morocco. *Water* **2023**, *15*, 130. [CrossRef]
13. Taoufiq, L.; Kacimi, I.; Saadi, M.; Nouayti, N.; Kassou, N.; Bouramtane, T.; El-Mouhdi, K. Assessment of Physicochemical and Bacteriological Parameters in the Angads Aquifer (Northeast Morocco): Application of Principal Component Analysis and Piper and Schoeller–Berkaloff Diagrams. *Appl. Environ. Soil Sci.* **2023**, *2023*, 2806854. [CrossRef]
14. Wang, B.; Wang, Y.; Wang, S. Improved water pollution index for determining spatiotemporal water quality dynamics: Case study in the Erdao Songhua River Basin, China. *Ecol. Indic.* **2021**, *129*, 107931. [CrossRef]
15. Zhang, M.; Chen, G.; Luo, Z.; Sun, X.; Xu, J. Spatial distribution, source identification, and risk assessment of heavy metals in seawater and sediments from Meishan Bay, Zhejiang coast, China. *Mar. Pollut. Bull.* **2020**, *156*, 111217. [CrossRef]
16. Zhang, H.; Yu, J.; Wang, P.; Wang, T.; Li, Y. Groundwater-fed oasis in arid Northwest China: Insights into hydrological and hydrochemical processes. *J. Hydrol.* **2021**, *597*, 126154. [CrossRef]

17. Zhang, Y.; Jia, R.; Wu, J.; Wang, H.; Luo, Z. Uncertain in WQI-based groundwater quality assessment methods: A case study in east of Beijing, China. *Environ. Earth Sci.* **2022**, *81*, 202. [CrossRef]
18. Uddin, M.G.; Nash, S.; Olbert, A.I. A review of water quality index models and their use for assessing surface water quality. *Ecol. Indic.* **2021**, *122*, 107218. [CrossRef]
19. Alexakis, D.E. Applying Factor Analysis and the CCME Water Quality Index for Assessing Groundwater Quality of an Aegean Island (Rhodes, Greece). *Geosciences* **2022**, *12*, 384. [CrossRef]
20. Atta, H.S.; Omar, M.A.-S.; Tawfik, A.M. Water quality index for assessment of drinking groundwater purpose case study: Area surrounding Ismailia Canal, Egypt. *J. Eng. Appl. Sci.* **2022**, *69*, 83. [CrossRef]
21. Vadiati, M.; Asghari-Moghaddam, A.; Nakhaei, M.; Adamowski, J.; Akbarzadeh, A. A fuzzy-logic based decision-making approach for identification of groundwater quality based on groundwater quality indices. *J. Environ. Manag.* **2016**, *184*, 255–270. [CrossRef]
22. Azzirgue, E.M.; Cherif, E.K.; Tchakoucht, T.A.; El Azhari, H.; Salmoun, F. Testing Groundwater Quality in Jouamaa Hakama Region (North of Morocco) Using Water Quality Indices (WQIs) and Fuzzy Logic Method: An Exploratory Study. *Water* **2022**, *14*, 3028. [CrossRef]
23. Azzirgue, E.M.; Salmoun, F.; Cherif, E.K.; Ait Tchakoucht, T.; Mejjad, N. Using Machine Learning Approaches to Predict Water Quality of Ibn Battuta Dam (Tangier, Morocco). In Proceedings of the 2nd International Conference on Big Data, Modelling and Machine Learning, Kenitra, Morocco, 15–16 July 2021; SCITEPRESS—Science and Technology Publications: Kenitra, Morocco, 2021; pp. 350–354.
24. Trabelsi, F.; Bel Hadj Ali, S. Exploring Machine Learning Models in Predicting Irrigation Groundwater Quality Indices for Effective Decision Making in Medjerda River Basin, Tunisia. *Sustainability* **2022**, *14*, 2341. [CrossRef]
25. Eid, M.H.; Elbagory, M.; Tamma, A.A.; Gad, M.; Elsayed, S.; Hussein, H.; Moghanm, F.S.; Omara, A.E.-D.; Kovács, A.; Péter, S. Evaluation of Groundwater Quality for Irrigation in Deep Aquifers Using Multiple Graphical and Indexing Approaches Sup-ported with Machine Learning Models and GIS Techniques, Souf Valley, Algeria. *Water* **2023**, *15*, 182. [CrossRef]
26. Uddin, G.; Nash, S.; Rahman, A.; Olbert, A.I. A sophisticated model for rating water quality. *Sci. Total. Environ.* **2023**, *868*, 161614. [CrossRef]
27. Zanial, W.N.C.W.; Malek, M.B.A.; Reba, M.N.M.; Zaini, N.; Ahmed, A.N.; Sherif, M.; Elshafie, A. River flow prediction based on improved machine learning method: Cuckoo Search-Artificial Neural Network. *Appl. Water Sci.* **2022**, *13*, 28. [CrossRef]
28. aldahy, D.H.; Ibrahim, M.A. Artificial Neural Networks Modelling for Al-Rustumiya Wastwater Treatment Plant in Baghdad. *3c Empresa Investig. Pensam. Crít.* **2023**, *12*, 257–271. [CrossRef]
29. Samson, S.; Elangovan, K. *Multivariate Statistical Analysis to Assess Groundwater Quality in Namakkal District, Tamil Nadu, India*; NISCAIR-CSIR: New Delhi, India, 2017.
30. Cherif, E.K.; Salmoun, F.; Nouayti, N.; da Silva, J.C.E. Determination of Physical-Chemical Quality of Tangier Free Zone and Gzenaya Zone Industrial Wastewaters (TFZ & GZ) in Tangier, Morocco. In Proceedings of the 4th Edition of International Conference on Geo-IT and Water Resources 2020, Geo-IT and Water Resources 2020, New York, NY, USA, 11 March 2020; ACM: Al-Hoceima, Morocco, 2020.
31. Ravikumar, P.; Somashekar, R.K. Principal component analysis and hydrochemical facies characterization to evaluate groundwater quality in Varahi river basin, Karnataka state, India. *Appl. Water Sci.* **2015**, *7*, 745–755. [CrossRef]
32. Güler, C.; Thyne, G.D.; McCray, J.E.; Turner, K.A. Evaluation of Graphical and Multivariate Statistical Methods for Classifi-cation of Water Chemistry Data. *Hydrogeol. J.* **2002**, *10*, 455–474. [CrossRef]
33. Khouni, I.; Louhichi, G.; Ghrabi, A. Use of GIS based Inverse Distance Weighted interpolation to assess surface water quality: Case of Wadi El Bey, Tunisia. *Environ. Technol. Innov.* **2021**, *24*, 101892. [CrossRef]
34. Etikala, B.; Golla, V.; Li, P.; Renati, S. Deciphering groundwater potential zones using MIF technique and GIS: A study from Tirupati area, Chittoor District, Andhra Pradesh, India. *Hydroresearch* **2019**, *1*, 1–7. [CrossRef]
35. Golla, V.; Arveti, N.; Etikala, B.; Sreedhar, Y.; Narasimhlu, K.; Harish, P. Data Sets on Spatial Analysis of Hydro Geochemistry of Gudur Area, SPSR Nellore District by Using Inverse Distance Weighted Method in Arc GIS 10.1. *Data Brief* **2019**, *22*, 1003–1011. [CrossRef]
36. Ohlert, P.L.; Bach, M.; Breuer, L. Accuracy assessment of inverse distance weighting interpolation of groundwater nitrate concentrations in Bavaria (Germany). *Environ. Sci. Pollut. Res.* **2022**, *30*, 9445–9455. [CrossRef]
37. Lahmar, M.; El Khodrani, N.; Omrania, S.; Dakak, H.; Douaik, A.; Iaaich, H.; El Azzouzi, M.; Mekkaoui, M.; Zouahri, A. As-sessement of the Physico-Chemical Quality of Groundwater in the Sidi Yahya Region, Gharb, Morocco. *Moroc. J. Chem.* **2019**, *7*, 424–430.
38. El Oumlouki, K.; Moussadek, R.; Douaik, A.; Iaaich, H.; Dakak, H.; Chati, M.T.; Ghanimi, A.; El Midaoui, A.; El Amrani, M.; Zouahri, A. Assessment of the Groundwater Salinity Used for Irrigation and Risks of Soil Degradation in Souss-Massa, Morocco. *Irrig. Drain.* **2018**, *67*, 38–51. [CrossRef]
39. El Mouine, Y.; El Hamdi, A.; Morarech, M.; Valles, V.; Yachou, H.; Dakak, H. Groundwater Contamination Due to Landfill Leachate—A Case Study of Tadla Plain. *Environ. Sci. Proc.* **2022**, *16*, 53. [CrossRef]
40. Chandran, S.; Selvan, P.; Dhanasekarapandian, M.; Kumar, V.; Surendran, U. Hydrogeochemical characteristics of surface and groundwater: Suitability for human consumption and irrigated agriculture purposes in Suruliyar sub basin, South India. *Environ. Geochem. Health* **2021**, *44*, 1713–1737. [CrossRef] [PubMed]

41. Zouahri, A.; Dakak, H.; Douaik, A.; El Khadir, M.; Moussadek, R. Evaluation of groundwater suitability for irrigation in the Skhirat region, Northwest of Morocco. *Environ. Monit. Assess.* **2014**, *187*, 4184. [CrossRef] [PubMed]
42. Yidana, S.M.; Yidana, A. Assessing water quality using water quality index and multivariate analysis. *Environ. Earth Sci.* **2009**, *59*, 1461–1473. [CrossRef]
43. Montcoudiol, N.; Molson, J.; Lemieux, J.M. Groundwater Geochemistry of the Outaouais Region (Québec, Canada): A Re-gional-Scale Study. *Hydrogeol. J.* **2015**, *23*, 377. [CrossRef]
44. Cloutier, V.; Lefebvre, R.; Therrien, R.; Savard, M.M. Multivariate statistical analysis of geochemical data as indicative of the hydrogeochemical evolution of groundwater in a sedimentary rock aquifer system. *J. Hydrol.* **2008**, *353*, 294–313. [CrossRef]
45. de la Hera-Portillo, Á.; López-Gutiérrez, J.; Moreno-Merino, L.; Llorente-Isidro, M.; Fensham, R.; Fernández, M.; Ghanem, M.; Salman, K.; Sánchez-Fabián, J.; Gallego-Rojas, N.; et al. Geodiversity of Las Loras UNESCO Global Geopark: Hydrogeological Significance of Groundwater and Landscape Interaction and Conceptual Model of Functioning. *Resources* **2023**, *12*, 14. [CrossRef]
46. Wali, S.U.; Alias, N.B.; Bin Harun, S.; Umar, K.J.; Gada, M.A.; Dankani, I.M.; Kaoje, I.U.; Usman, A.A. Water quality indices and multivariate statistical analysis of urban groundwater in semi-arid Sokoto Basin, Northwestern Nigeria. *Groundw. Sustain. Dev.* **2022**, *18*, 100779. [CrossRef]
47. Jassas, H.; Merkel, B. Assessment of hydrochemical evolution of groundwater and its suitability for drinking and irrigation purposes in Al-Khazir Gomal Basin, Northern Iraq. *Environ. Earth Sci.* **2015**, *74*, 6647–6663. [CrossRef]
48. Alkinani, M.; Merkel, B. Hydrochemical and isotopic investigation of groundwater of Al-Batin alluvial fan aquifer, Southern Iraq. *Environ. Earth Sci.* **2017**, *76*, 301. [CrossRef]
49. Kumar, B.; Singh, U.K.; Ojha, S.N. Evaluation of geochemical data of Yamuna River using WQI and multivariate statistical analyses: A case study. *Int. J. River Basin Manag.* **2018**, *17*, 143–155. [CrossRef]
50. Kumar, M.; Ramanathan, A.; Keshari, A.K. Understanding the extent of interactions between groundwater and surface water through major ion chemistry and multivariate statistical techniques. *Hydrol. Process.* **2008**, *23*, 297–310. [CrossRef]
51. Danczak, R.E.; Sawyer, A.H.; Williams, K.H.; Stegen, J.C.; Hobson, C.; Wilkins, M.J. Seasonal hyporheic dynamics control coupled microbiology and geochemistry in Colorado River sediments. *J. Geophys. Res. Biogeosciences* **2016**, *121*, 2976–2987. [CrossRef]
52. Harjung, A.; Perujo, N.; Butturini, A.; Romaní, A.M.; Sabater, F. Responses of microbial activity in hyporheic pore water to biogeochemical changes in a drying headwater stream. *Freshw. Biol.* **2019**, *64*, 735–749. [CrossRef]
53. Yuan, R.; Wang, M.; Wang, S.; Song, X. Water transfer imposes hydrochemical impacts on groundwater by altering the interaction of groundwater and surface water. *J. Hydrol.* **2020**, *583*, 124617. [CrossRef]
54. Vrzel, J.; Solomon, D.K.; Blažeka, Ž.; Ogrinc, N. The study of the interactions between groundwater and Sava River water in the Ljubljansko polje aquifer system (Slovenia). *J. Hydrol.* **2018**, *556*, 384–396. [CrossRef]
55. Rugel, K.; Golladay, S.W.; Jackson, C.R.; Rasmussen, T.C. Delineating groundwater/surface water interaction in a karst watershed: Lower Flint River Basin, southwestern Georgia, USA. *J. Hydrol. Reg. Stud.* **2016**, *5*, 1–19. [CrossRef]
56. Rozemeijer, J.; Klein, J.; Hendriks, D.; Borren, W.; Ouboter, M.; Rip, W. Groundwater-surface water relations in regulated lowland catchments; hydrological and hydrochemical effects of a major change in surface water level management. *Sci. Total. Environ.* **2019**, *660*, 1317–1326. [CrossRef]
57. Kshetrimayum, K.; Laishram, P. Assessment of surface water and groundwater interaction using hydrogeology, hydrochemical and isotopic constituents in the Imphal river basin, Northeast India. *Groundw. Sustain. Dev.* **2020**, *11*, 100391. [CrossRef]
58. Kong, F.; Song, J.; Zhang, Y.; Fu, G.; Cheng, D.; Zhang, G.; Xue, Y. Surface Water-Groundwater Interaction in the Guanzhong Section of the Weihe River Basin, China. *Groundwater* **2018**, *57*, 647–660. [CrossRef]
59. Menció, A.; Galán, M.; Boix, D.; Mas-Pla, J. Analysis of stream–aquifer relationships: A comparison between mass balance and Darcy's law approaches. *J. Hydrol.* **2014**, *517*, 157–172. [CrossRef]
60. Martinez, J.L.; Raiber, M.; Cox, M.E. Assessment of groundwater–surface water interaction using long-term hydrochemical data and isotope hydrology: Headwaters of the Condamine River, Southeast Queensland, Australia. *Sci. Total. Environ.* **2015**, *536*, 499–516. [CrossRef]
61. Yang, N.; Zhou, P.; Wang, G.; Zhang, B.; Shi, Z.; Liao, F.; Li, B.; Chen, X.; Guo, L.; Dang, X.; et al. Hydrochemical and isotopic interpretation of interactions between surface water and groundwater in Delingha, Northwest China. *J. Hydrol.* **2021**, *598*, 126243. [CrossRef]
62. Fadili, A.; Mehdi, K.; Riss, J.; Najib, S.; Makan, A.; Boutayab, K. Evaluation of groundwater mineralization processes and seawater intrusion extension in the coastal aquifer of Oualidia, Morocco: Hydrochemical and geophysical approach. *Arab. J. Geosci.* **2015**, *8*, 8567–8582. [CrossRef]
63. Nouayti, N.; Cherif, E.K.; Algarra, M.; Pola, M.L.; Fernández, S.; Nouayti, A.; Esteves da Silva, J.C.; Driss, K.; Samlani, N.; Mohamed, H.; et al. Determination of Physicochemical Water Quality of the Ghis-Nekor Aquifer (Al Hoceima, Morocco) Using Hydrochemistry, Multiple Isotopic Tracers, and the Geographical Information System (GIS). *Water* **2022**, *14*, 606. [CrossRef]
64. Ouhamdouch, S. Hydrogeochemical processes in rural coastal aquifer (Haha region, Morocco). *Environ. Sci. Pollut. Res.* **2023**, *30*, 43975–43990. [CrossRef] [PubMed]
65. Ghalit, M.; Bouaissa, M.; Gharibi, E.; Taupin, J.-D.; Patris, N. Hydrogeochemical Characteristics and Isotopic Tools Used to Identify the Mineralization Processes of Bottled Mineral Water in Morocco. *Geosciences* **2023**, *13*, 38. [CrossRef]

66. Ez-Zaouy, Y.; Bouchaou, L.; Schreiber, H.; Montcoudiol, N.; Kalberkamp, U.; Danni, S.O.; Touab, A.; Abourrig, F.; Hssaisoune, M. Combined geophysical methods to investigate seawater intrusion in the Souss-Massa coastal area, Morocco. *Groundw. Sustain. Dev.* **2023**, *21*, 100915. [CrossRef]
67. El Ouali, A.; Roubil, A.; Lahrach, A.; Moudden, F.; Ouzerbane, Z.; Hammani, O.; El Hmaidi, A. Assessment of groundwater quality and its recharge mechanisms using hydrogeochemical and isotopic data in the Tafilalet plain (south-eastern Morocco). *Mediterr. Geosci. Rev.* **2023**, *5*, 1–14. [CrossRef]
68. El Yousfi, Y.; Himi, M.; El Ouarghi, H.; Aqnouy, M.; Benyoussef, S.; Gueddari, H.; Hmeid, H.A.; Alitane, A.; Chaibi, M.; Zahid, M.; et al. Assessment and Prediction of the Water Quality Index for the Groundwater of the Ghiss-Nekkor (Al Hoceima, Northeastern Morocco). *Sustainability* **2022**, *15*, 402. [CrossRef]
69. Kacem, L.; Agoussine, M.; Igmoullan, B.; Mokhtari, S.; Amar, H. Features of interaction between lake water and springs, and evaluation of hydrochemical composition of water in Ifni Lake (High Atlas Mountains, Morocco, north of Africa). *Water Resour.* **2016**, *43*, 395–401. [CrossRef]
70. Haut Commissariat au Plan Direction Régionale de Tanger-Tétouan-Al Hoceima. *Note d'information Sur Les Comptes Régio-naux En2019*; Haut Commissariat au Plan Direction Régionale de Tanger-Tétouan-Al Hoceima: Tangier, Morocco, 2021.
71. Tribak, Y.; El Morabiti, K.; Hlila, R. TEtude Hydrogéologique Préliminaire de La Zone Des Flyschs à l'Ouest de Tétouan (Maroc). *Int. J. Innov. Appl. Stud.* **2016**, *14*, 653.
72. Mahamat, S.A.M.; Maoudombaye, T.; Abdelsalam, T.; Ndoumtamia, G.; Loukhman, B. Évaluation de la qualité physico-chimique des eaux d'adduction publique de la Société Tchadienne des Eaux à N'djamena au Tchad. *J. Appl. Biosci.* **2016**, *95*, 8973. [CrossRef]
73. Tiwari, A.K.; Singh, P.K.; Mahato, M.K. GIS-Based Evaluation of Water Quality Index of Ground Water Resources in West Bokaro Coalfield, India. *Curr. World Environ.* **2014**, *9*, 843. [CrossRef]
74. Barakat, A.; Hilali, A.; El Baghdadi, M.; Touhami, F. Assessment of shallow groundwater quality and its suitability for drinking purpose near the Béni-Mellal wastewater treatment lagoon (Morocco). *Hum. Ecol. Risk Assess. Int. J.* **2019**, *26*, 1476–1495. [CrossRef]
75. *NM 03.7.001*; Norme Marocaine Relative à La Qualité Des Eaux d'alimentation Humaine. Bulletin Officiel: Rabat, Morocco, 2006.
76. Ustaoğlu, F.; Tepe, Y.; Taş, B. Assessment of stream quality and health risk in a subtropical Turkey river system: A combined approach using statistical analysis and water quality index. *Ecol. Indic.* **2019**, *113*, 105815. [CrossRef]
77. Xiao, Y.; Liu, K.; Hao, Q.; Xiao, D.; Zhu, Y.; Yin, S.; Zhang, Y. Hydrogeochemical insights into the signatures, genesis and sustainable perspective of nitrate enriched groundwater in the piedmont of Hutuo watershed, China. *Catena* **2022**, *212*, 106020. [CrossRef]
78. Soumaila, K.I.; Mustapha, N.; Mohamed, C. Assessment of Surface Water Quality using Indices and Geographic Information System in the Sebou River Basin, Morocco. *Eur. Sci. J. ESJ* **2021**, *17*, 249. [CrossRef]
79. Benamar, A.; Mahjoubi, F.Z.; Kzaibe, F. Evaluation of Water Quality of Oum Er Rbia River (Morocco) Using Water Quality Index (WQI) Method. *J. Appl. Surf. Interfaces* **2019**, *5*. [CrossRef]
80. Olurin, O.; Ganiyu, S.; Ogunsanwo, F.; Ojo, A.O.; Alabi, A.; Adegbamigbe, O. Groundwater quality assessments around acassava processing mill on the sedimentary terrain of Ilaro, South-western Nigeria. *Hydroresearch* **2022**, *5*, 108–117. [CrossRef]
81. Shankar, B.S.; Sanjeev, L. Assessment of Water Quality Index for the Groundwaters of an Industrial Area In Bangalore, India. *Environ. Eng. Sci.* **2008**, *25*, 911–916. [CrossRef]
82. Knopek, T.; Dabrowska, D. The Use of the Contamination Index and the LWPI Index to Assess the Quality of Groundwater in the Area of a Municipal Waste Landfill. *Toxics* **2021**, *9*, 66. [CrossRef]
83. Krishan, G.; Kumar, M.; Rao, M.S.; Garg, R.; Yadav, B.K.; Kansal, M.; Singh, S.; Bradley, A.; Muste, M.; Sharma, L. Integrated approach for the investigation of groundwater quality through hydrochemistry and water quality index (WQI). *Urban Clim.* **2023**, *47*, 101383. [CrossRef]
84. Kadam, A.; Wagh, V.; Jacobs, J.; Patil, S.; Pawar, N.; Umrikar, B.; Sankhua, R.; Kumar, S. Integrated approach for the evaluation of groundwater quality through hydro geochemistry and human health risk from Shivganga river basin, Pune, Maharashtra, India. *Environ. Sci. Pollut. Res.* **2021**, *29*, 4311–4333. [CrossRef]
85. Li, C.; Gao, Z.; Chen, H.; Wang, J.; Liu, J.; Li, C.; Teng, Y.; Liu, C.; Xu, C. Hydrochemical analysis and quality assessment of groundwater in southeast North China Plain using hydrochemical, entropy-weight water quality index, and GIS techniques. *Environ. Earth Sci.* **2021**, *80*, 523. [CrossRef]
86. Akhtar, N.; Ishak, M.; Ahmad, M.; Umar, K.; Yusuff, M.M.; Anees, M.; Qadir, A.; Almanasir, Y.A. Modification of the Water Quality Index (WQI) Process for Simple Calculation Using the Multi-Criteria Decision-Making (MCDM) Method: A Review. *Water* **2021**, *13*, 905. [CrossRef]
87. Mukherjee, I.; Singh, U.K.; Chakma, S. Evaluation of groundwater quality for irrigation water supply using multi-criteria decision-making techniques and GIS in an agroeconomic tract of Lower Ganga basin, India. *J. Environ. Manag.* **2022**, *309*, 114691. [CrossRef]
88. Batarseh, M.; Imreizeeq, E.; Tilev, S.; Al Alaween, M.; Suleiman, W.; Al Remeithi, A.M.; Al Tamimi, M.K.; Al Alawneh, M. Assessment of groundwater quality for irrigation in the arid regions using irrigation water quality index (IWQI) and GIS-Zoning maps: Case study from Abu Dhabi Emirate, UAE. *Groundw. Sustain. Dev.* **2021**, *14*, 100611. [CrossRef]

89. Mahammad, S.; Hoque, M.; Islam, A.; Majumder, A. Assessment of groundwater quality for irrigation purposes: A case study of Hooghly District, West Bengal, India. In *Case Studies in Geospatial Applications to Groundwater Resources*; Elsevier: Amsterdam, The Netherlands, 2023; pp. 289–314. [CrossRef]
90. Wilcox, L. *Classification and Use of Irrigation Waters (No. 969)*; US Department of Agriculture: Washington, DC, USA, 1955.
91. Alsubih, M.; Mallick, J.; Islam, A.R.M.T.; Almesfer, M.K.; Ben Kahla, N.; Talukdar, S.; Ahmed, M. Assessing Surface Water Quality for Irrigation Purposes in Some Dams of Asir Region, Saudi Arabia Using Multi-Statistical Modeling Approaches. *Water* **2022**, *14*, 1439. [CrossRef]
92. Samtio, M.S.; Hakro, A.A.A.D.; Jahangir, T.M.; Mastoi, A.S.; Lanjwani, M.F.; Rajper, R.H.; Lashari, R.A.; Agheem, M.H.; Noonari, M.W. Impact of rock-water interaction on hydrogeochemical characteristics of groundwater: Using multivariate statistical, water quality index and irrigation indices of chachro sub-district, thar desert, sindh, Pakistan. *Groundw. Sustain. Dev.* **2023**, *20*, 100878. [CrossRef]
93. Richards, L. Diagnosis and improvement of saline and alkali soils. *Soil Sci.* **1954**, *78*, 154. [CrossRef]
94. Eaton, F.M. Significance of Carbonates in Irrigation Waters. *Soil Sci.* **1950**, *69*, 123–134. [CrossRef]
95. Doneen, L. *Notes on Water Quality in Agriculture*; Department of Water Sciences and Engineering, University of California: Davis, CA, USA, 1964.
96. Kelley, W.P. Use of Saline Irrigation Water. *Soil Sci.* **1963**, *95*, 385–391. [CrossRef]
97. Gupta, S.K.; Gupta, I.C. *Management of Saline Soils and Waters*; Oxford & IBH Publishing, Co.: New Delhi, India, 1987.
98. Paliwal, K.V. *; Indian Agricultural Research Institute. Irrigation with Saline Water*; New Delhi (India) IARI, Water Technology Centre: New Delhi, India, 1972.
99. Backhaus, K.; Erichson, B.; Gensler, S.; Weiber, R.; Weiber, T. Cluster Analysis. In *Multivariate Analysis: An Application-Oriented Introduction*; Backhaus, K., Erichson, B., Gensler, S., Weiber, R., Weiber, T., Eds.; Springer Fachmedien: Wiesbaden, Germany, 2021; pp. 451–530. ISBN 978-3-658-32589-3.
100. Shyamala, G.; Sree Sakthi Engineering College; Jeyanthi, J. Integrated Weighted Overlay Model Using Inverse Distance Weightage for Assessing Groundwater Quality. *J. Environ. Sci. Manag.* **2019**, *20*, 26–32. [CrossRef]
101. Ogbozige, F.J.; Adie, D.B.; Abubakar, U.A. Water quality assessment and mapping using inverse distance weighted interpolation: A case of River Kaduna, Nigeria. *Niger. J. Technol.* **2018**, *37*, 249. [CrossRef]
102. Yadav, K.K.; Gupta, N.; Kumar, V.; Choudhary, P.; Khan, S.A. GIS-based evaluation of groundwater geochemistry and statistical determination of the fate of contaminants in shallow aquifers from different functional areas of Agra city, India: Levels and spatial distributions. *RSC Adv.* **2018**, *8*, 15876–15889. [CrossRef]
103. Bon, A.F.; Ngoss, T.A.M.N.; Mboudou, G.E.; Banakeng, L.A.; Ngoupayou, J.R.N.; Ekodeck, G.E. Groundwater flow patterns, hydrogeochemistry and metals background levels of shallow hard rock aquifer in a humid tropical urban area in sub-Saharan Africa- A case study from Olézoa watershed (Yaoundé-Cameroon). *J. Hydrol. Reg. Stud.* **2021**, *37*, 100904. [CrossRef]
104. Aladejana, J.A.; Kalin, R.M.; Sentenac, P.; Hassan, I. Groundwater quality index as a hydrochemical tool for monitoring saltwater intrusion into coastal freshwater aquifer of Eastern Dahomey Basin, Southwestern Nigeria. *Groundw. Sustain. Dev.* **2021**, *13*, 100568. [CrossRef]
105. Badmus, G.; Ogungbemi, O.; Enuiyin, O.; Adeyeye, J.; Ogunyemi, A. Delineation of leachate plume migration and appraisal of heavy metals in groundwater around Emirin dumpsite, Ado-Ekiti, Nigeria. *Sci. Afr.* **2022**, *17*, e01308. [CrossRef]
106. Zemour, Y.; Mebrouk, N.; Mayer, A.; Mekebret, I.; Sherif, M.I. Hydrochemical and geological controls on dissolved radium and radon in northwestern Algeria hydrothermal groundwaters. *Chemosphere* **2023**, *313*, 137573. [CrossRef]
107. Mladenov, N.; Parsons, D.; Kinoshita, A.M.; Pinongcos, F.; Mueller, M.; Garcia, D.; Lipson, D.A.; Grijalva, L.M.; Zink, T.A. Groundwater-surface water interactions and flux of organic matter and nutrients in an urban, Mediterranean stream. *Sci. Total. Environ.* **2021**, *811*, 152379. [CrossRef] [PubMed]
108. Osiakwan, G.M.; Appiah-Adjei, E.K.; Kabo-Bah, A.T.; Gibrilla, A.; Anornu, G. Assessment of groundwater quality and the controlling factors in coastal aquifers of Ghana: An integrated statistical, geostatistical and hydrogeochemical approach. *J. Afr. Earth Sci.* **2021**, *184*, 104371. [CrossRef]
109. Fu, T.; Li, C.; Wang, Z.; Qi, C.; Chen, G.; Fu, Y.; Su, Q.; Xu, X.; Liu, W.; Yu, H. Hydrochemical characteristics and quality assessment of groundwater in Guangxi coastal areas, China. *Mar. Pollut. Bull.* **2023**, *188*, 114564. [CrossRef]
110. Piper, A.M. A graphic procedure in the geochemical interpretation of water-analyses. *Eos Trans. Am. Geophys. Union* **1944**, *25*, 914–928. [CrossRef]
111. Upchurch, S.; Scott, T.M.; Alfieri, M.C.; Fratesi, B.; Dobecki, T.L. Hydrogeochemistry of Florida Karst Waters. In *The Karst Systems of Florida; Cave and Karst Systems of the World*; Springer International Publishing: Cham, Switzerland, 2019; pp. 145–206. ISBN 978-3-319-69634-8.
112. Schoeller, H. Geochemistry of Groundwater. In *Groundwater Studies–An International Guide for Research and Practice*; Brown, R.H., Konoplyantsev, A.A., Ineson, J., Kovalevsky, V.S., Eds.; UNESCO: Paris, French, 1977; pp. 1–18.
113. Gueddari, H.; Akodad, M.; Baghour, M.; Moumen, A.; Skalli, A.; El Yousfi, Y.; Ismail, A.; Chahban, M.; Azizi, G.; Hmeid, H.A.; et al. The salinity origin and hydrogeochemical evolution of groundwater in the Oued Kert basin, north-eastern of Morocco. *Sci. Afr.* **2022**, *16*, e01226. [CrossRef]
114. World Health Organization. *Guidelines for Drinking Water Quality–Fourth Edition Incorporating the First Addendum*; World Health Organization: Geneva, Switzerland, 2017.

115. Chen, D.; Elhadj, A.; Xu, H.; Xu, X.; Qiao, Z. A Study on the Relationship between Land Use Change and Water Quality of the Mitidja Watershed in Algeria Based on GIS and RS. *Sustainability* **2020**, *12*, 3510. [CrossRef]
116. Ramakrishnaiah, C.R.; Sadashivaiah, C.; Ranganna, G. Assessment of Water Quality Index for the Groundwater in Tumkur Taluk, Karnataka State, India. *E-J. Chem.* **2009**, *6*, 523–530. [CrossRef]
117. Ismail, E.; Abdelhalim, A.; Heleika, M.A. Hydrochemical characteristics and quality assessment of groundwater aquifers northwest of Assiut district, Egypt. *J. Afr. Earth Sci.* **2021**, *181*, 104260. [CrossRef]
118. Kothari, V.; Vij, S.; Sharma, S.; Gupta, N. Correlation of various water quality parameters and water quality index of districts of Uttarakhand. *Environ. Sustain. Indic.* **2020**, *9*, 100093. [CrossRef]
119. Nong, X.; Shao, D.; Xiao, Y.; Zhong, H. Spatio-Temporal Characterization Analysis and Water Quality Assessment of the South-to-North Water Diversion Project of China. *Int. J. Environ. Res. Public Health* **2019**, *16*, 2227. [CrossRef] [PubMed]
120. Xu, S.; Frey, S.; Erler, A.; Khader, O.; Berg, S.; Hwang, H.; Callaghan, M.; Davison, J.; Sudicky, E. Investigating groundwater-lake interactions in the Laurentian Great Lakes with a fully-integrated surface water-groundwater model. *J. Hydrol.* **2021**, *594*, 125911. [CrossRef]
121. El Osta, M.; Masoud, M.; Alqarawy, A.; Elsayed, S.; Gad, M. Groundwater Suitability for Drinking and Irrigation Using Water Quality Indices and Multivariate Modeling in Makkah Al-Mukarramah Province, Saudi Arabia. *Water* **2022**, *14*, 483. [CrossRef]